Plant Physiology Preview. Published on January 15, 2016, as DOI:10.1104/pp.15.01679

DUPLICATED GENOME REPROGRAMS ENERGY WILLOW GROWTH

Corresponding author: Dénes Dudits

Institute of Plant Biology

Biological Research Center, Hungarian Academy of Sciences

6726 Szeged, Temesvári kr. 62 Hungary

Tel.: 36 62 599-600

dudits.denes@brc.mta.hu

Research Area: Genes, Development and Evolution

.

RESPONSE OF ORGAN STRUCTURE AND PHYSIOLOGY TO AUTOTETRAPLOIDIZATION IN EARLY DEVELOPMENT OF ENERGY WILLOW *Salix viminalis* L.

Dénes Dudits[1], Katalin Török[1], András Cseri[1], Kenny Paul[1], Anna V. Nagy[1], Bettina Nagy[1], László Sass[1], Györgyi Ferenc[1], Radomira Vankova[2], Petre Dobrev[2], Imre Vass[1] and Ferhan Ayaydin[1]

1. Institute of Plant Biology, Biological Research Centre, H.A.S. Szeged, Hungary
2. Institute of Experimental Botany, AS CR Prague, Czech Republic

Summary

Enlarged leaf size, stem diameter and root system of autotetraploid energy willows are associated with changes in hormonal status and efficiency of photosynthesis.

Footnotes:

This work was partly supported by a grant from European Plant Phenotyping Network (EPPN) grant agreement no. 284443. Construction of the root phenotyping instrument was supported by GOP-1.1.1-11-2012-0365 grant.

Corresponding author email: dudits.denes@brc.mta.hu

.

Abstract

Biomass productivity of the energy willow as a short rotation woody crop depends on organ structure and functions that are under the control of genome size. Colchicine treatment of axillary buds resulted in a set of autotetraploid *Salix viminalis* var. Energo genotypes (Polyploid Energo, PP-E; 2n=4x=76) with variation in the green pixel-based shoot surface area. In cases where increased shoot biomass was observed, it was primarily derived from larger leaf size and wider stem diameter. Autotetraploidy slowed down primary growth and increased shoot diameter (a parameter of secondary growth). The duplicated genome size enlarged bark and wood layers in twigs sampled in the field. The PP-E plants developed wider leaves with thicker midrib and enlarged palisade parenchyma cells. Autotetraploid leaves contained significantly increased amounts of active gibberellins, cytokinins, salicylic acid and jasmonate, as compared to diploid individuals. Greater net photosynthetic CO_2 uptake was detected in leaves of PP-E plants with increased chlorophyll and carotenoid content. Improved photosynthetic functions in tetraploids were also shown by more efficient electron transport rates of Photosystems I and II. Autotetraploidization increased biomass of the root system of PP-E plants relative to diploids. Sections of tetraploid roots showed thickening with enlarged cortex cells. Elevated amounts of indole-acetic acid, active cytokinins, active gibberellin and salicylic acid were detected in the root tips of these plants. The presented variation in traits of tetraploid willow genotypes provides a basis to use autopolyploidization as chromosome engineering technique for altering organ development of energy plants in order to improve biomass productivity.

.

INTRODUCTION

Energy security and climate change as global problems urge increased efforts to use of plants as renewable energy sources both for power generation and transportation fuel production. Selected wood species, such as willows (*Salix* spp.) can be cultivated as short rotation coppice (SRC) for rapid accumulation of biomass and reduction of carbon dioxide emission. Coppicing reinvigorates shoot growth, resulting in a special woody plant life cycle that differs from natural tree development, which takes decades. In this cultivation system small stem cuttings are planted at high densities (15000-25000/ha). In the soil, these dormant wood cuttings first produce roots and shoots that emerge from reactivated buds. During the first year, the growing shoots mature to woody stems. In the winter, these stems are cut back and in the following spring the cut stumps develop multiple shoots. The SRC plantations are characterized by a very short, two- to three-year rotation and the most productive varieties can produce up to 15 tonnes of oven-dried wood per hectare per year (Cunniff and Cerasuolo, 2011). The high-density willow plantations can also be efficiently used for heavy metal or organic phytoremediation as reviewed by Marmiroli et al., (2011).

The biomass productivity of shrub willows is largely dependent on coppicing capability, early vigorous growth, shoot growth rate and final stem height, root system size, photosynthetic efficiency, formation and composition of woody stems, water and nutrient use as well as abiotic and biotic stress tolerance. Genetic improvement of all these traits can be based on broad natural genetic resources represented by more than 400 species in the genus *Salix*. More than 200 species have hybrid origin and ploidy levels vary from diploid up to dodecaploid (Suda and Argus, 1968; Newsholme, 1992). In addition to molecular marker-assisted clone selection, intra- and interspecific crosses have been shown to further extend genetic variability in breeding programs for biomass yield (Karp et al., 2011).

.

During natural diversification and artificial crossings of *Salix* species, the willow genomes frequently undergo polyploidization resulting in triploid or tetraploid allopolyploids. In triploid hybrids, both heterosis and ploidy can contribute to the improved biomass yield (Serapiglia et al., 2014). While the alloploid triploids have attracted considerable attention in willow improvement, the potentials of autotetraploid willow genotypes have not been exploited so far**.** As it was shown for other short-rotation wood species (poplar, black locust, Paulownia, birch), doubling the chromosome set by colchicine treatment can cause significant changes in organ morphology or growth parameters (Tang et al., 2010; Cai and Kang, 2011; Harbard et al., 2012; Mu et al., 2012; Wang et al., 2013). In several polyploidization protocols, the *in vitro* cultured tissues are exposed to different doses of colchicine or other inhibitors of mitotic microtubule function, and plantlets are differentiated from polyploid somatic cells (Tang et al., 2010; Cai and Kang, 2011). Alternatively, seeds or apical meristems of germinating seedlings can be treated with a colchicine solution (Harbard et al., 2012). Allotetraploids of poplar were produced by zygotic chromosome doubling that was induced by colchicine and high temperature treatment (Wang et al., 2013).

Since tetraploid willow plants with 2n= 4x =76 chromosomes are expected to represent novel genetic variability especially for organ development and physiological parameters, a polyploidization project was initiated that was based on a highly productive diploid energy willow variety, 'Energo'. Colchicine treatment of reactivated axillary buds of the *in vitro* grown energy willow plantlets resulted in autotetraploid shoots and subsequently plants. For comparison of diploid and tetraploid variants of willow plants, digital imaging of green organs and roots was used for phenotyping. Among the tetraploid lines, genotypes were identified with improved biomass production, better photosynthetic parameters, altered organ structure and hormone composition. The new tetraploid willow variants produced can serve as a unique experimental material for uncovering key factors in biomass production in this short-rotation energy plant. In the future, these plants can also serve as crossing partners of diploid lines for the production of novel triploid energy willow genotypes.

RESULTS

Production of autotetraploid willow plants by colchicine-treatment of axillary buds *in vitro*

.

Autotetraploid genotypes were produced by colchicine treatment of auxiliary bud meristems of willow plantlets cultured in MS agar medium (see Materials and Methods). Several plantlets could be recovered after the treatment**.** These plantlets were grown and propagated in agar cultures. For early screening of DNA ploidy level, nuclei were isolated from root tips of stem cuttings for flow cytometric determination (Fig. 1). As shown by the histograms of flow cytometric analysis, plants of PP-E lines have doubled DNA content in their root cells. These results were confirmed by chromosome counting using fluorescence microscopy (Fig. 1). Diploid Energo plants have a karyotype with 2n=2x=38 chromosomes. Sixteen lines with 2n=4x=76 chromosomes was identified by these tests. Plants with mixoploid root tissues were discarded. Both tetraploid and control diploid plantlets were transferred into soil and grown in the greenhouse. These plants were propagated by stem cuttings after rooting in water. At this step the ploidy level was also checked by flow cytometry using nuclei isolated from roots. Screening and selection of lines with stable tetraploid nature were continued during propagation. Stem cuttings were also planted in the field, which allowed analyses of shoot regrowth under native environmental conditions. Independent tetraploid plantlets identified in *in vitro* cultures served as starting material for establishment of tetraploid lines transferred to the soil in the greenhouse. In subsequent comparison of diploid and tetraploid plants, several lines were used according to the availability of proper plant material.

Phenotyping green shoot surface area during early growth of diploid and tetraploid energy willow plants

Based on studies with various plant species (Tackenberg et al. 2007, Golzarian et al., 2011, Fehér-Juhász et al., 2014) green pixel values reflecting leaf/shoot surface area are assumed to be directly proportional to green mass of plants and they can be used for comparison of different genotypes. Dormant stem cuttings were planted in soil-containing special pots used in a phenotyping platform operating under controlled greenhouse conditions. Shoot development was monitored by digital photography providing the green pixel-based average shoot surface area. As shown in Fig. 2A, the analyzed tetraploid lines exhibited moderate differences in growth

.

characteristics. Average values of shoot surface areas for PP-E2 and PP-E10 plants were higher than those for diploid plants at each sampling point during the 7 week experiment. PP-E13 plants, however, displayed lower average values for shoot surface area when compared to diploid plants. These statistically non-significant differences in green pixel number of shoots may arise from several factors such as shoot length, stem diameter, leaf number, leaf size and petiole shape. Therefore a detailed comparison of these organs from diploid and tetraploid plants was carried out under greenhouse and under field conditions.

At the end of the seven-week phenotyping study, shoot length measurement showed 20-25% reduction in primary shoot length of tetraploid plants relative to the diploid ones (Fig. 2B, Fig 3). This shortening of the shoot length was linked to the enhanced secondary growth of shoots that resulted in significantly wider stem diameters in several tetraploid genotypes such as PP-E2, PP-E7 and PP-E13 (Fig. 2C, based on Welch's *t*-test). Box-plot analysis revealed considerable variation in these parameters between individuals of the same autotetraploid genotype.

Growth characteristics observed in the greenhouse were also scored by monitoring shoot growth under field conditions in spring during re-growth of shoots from dormant buds. As shown by Table I, primary growth of all the tested tetraploid variants was reduced in comparison to the diploid plants. As a general trend, autotetraploidy slowed down primary growth during the early shoot development of willow plants. To assess secondary growth characteristics, shoot diameters of the same plants were also measured (Table I). Without exception, plants of the tetraploid lines developed thicker stems in average. Selected genotypes (PP-E3; PP-E12; PP-E13) showed statistically significant increases in secondary growth. The enlarged stem diameter of willow plants from several tetraploid genotypes (Fig. 2C; Fig. 4; Table I) can be related to substantial anatomical alterations as a consequence of doubled genome size. Cross-sections of stems from older stem regions of willow plants revealed that wood formation between the primary and secondary xylem rings was increased significantly in the tested tetraploid plants relative to diploid plants. The bark region was also thicker in stems of the tetraploid plants than in diploid control ones (Fig. 4).

The doubled chromosome set alters shape, size, ultrastructure and hormone composition of willow leaves

.

The phenotyping experiment demonstrated that the autotetraploid willow plants developed larger foliage (Fig. 3). Enlargement of leaves can originate from a set of characteristic changes at the cellular level. The tetraploid plants produced significantly broader leaves than the diploid ones (Fig. 5, A and B). The width of leaf lamina was doubled in plants of tetraploid genotypes. Leaf lengths either increased or decreased moderately, varying among plants with various genotypes (Fig. 5, A and C). The cumulative effect of these size differences was reflected as a general trend of increased total leaf biomass for tetraploid plants (Fig. 5D).

Cross-section analysis of leaf midribs revealed an increase in the vein-xylem area in tetraploid leaves with enlarged leaf-lamina (Fig. 6). Plants from all the studied tetraploid lines developed significantly thicker midribs. This anatomical feature was the most prominent in PP-E 7 plants which displayed an average cross sectional area $0.72 \times 10^6 \mu m^2$. This value was twice as big as that of diploid samples ($0.33 \times 10^6 \mu m^2$).

Beyond the described alterations in leaf morphology, major modifications at the cellular level were also detected by cytological analyses of leaf cross sections. The tetraploid palisade parenchyma cells were by 50% larger than the diploids as quantified by the cross sectional area measurements (Fig. 7B). Due to this increase in cell size, fewer tetraploid cells were found per unit distance (100 μm) along the parenchyma layer (Fig. 7C).

Several significant differences as compared to diploid leaves were recognized in the cellular and organ structure of leaves of the tetraploid willow plants. These changes may have originated from an altered hormonal status of these leaves. Concentrations of the major plant hormones were compared in young expanded leaves of control diploid and selected tetraploid lines (Table II). The youngest fully developed leaves were compared in order to avoid the potential effect of different rate of leaf development among individual lines. The levels of active cytokinins (the sum of *trans*-zeatin, isopentenyladenine, *cis*-zeatin and dihydrozeatin and the corresponding ribosides) differed among individual tetraploid lines, being either higher or lower than the corresponding value for control diploid samples. However, the concentration of the most physiologically active cytokinin, *trans*-zeatin was enhanced in all tetraploid lines, and this increase, was statistically significant in the case of the PP-E6 line. Substantially increased levels of cytokinin N-glucosides in all tested tetraploid plants indicates enhanced deactivation of active

.

cytokinins and thus their higher turn-over in tetraploids. The most dramatic increase was detected in gibberellins, namely in active gibberellins GA_4 and GA_7 (expressed as pmol per g fresh weight). The tetraploid leaves contained 4.10-5.89 times higher levels of GA_4. Two out of three tetraploid lines (PP-E7 and PP-E13) had GA_7 contents elevated by 57–75 %. The concentrations of two stress hormones, salicylic acid and jasmonic acid were almost doubled in the leaves of some autotetraploid genotypes as compared to diploids. Differences in abscisic acid and indole-3-acetic acid contents were much less pronounced between diploid and tetraploid lines.

In relation to the above described fundamental differences in leaf anatomy and shape between diploid and tetraploid genotypes, alterations in water metabolism may also be impacted after genome duplication. Tetraploid willow leaves were characterized by elevated stomata conductance values (Fig. 8). Increased water utilization was characteristic for the majority of tetraploid plants. The stomata size of the tetraploid plants showed considerable variation. Enlarged stomata could be identified in certain genotypes (PP-E6: 27.55±2.33 μm and PP-E7: 23.24±1.84 μm) in comparison to the diploid plants (21.31±2.10 μm).

The autotetraploid energy willow genotypes show improved net photosynthetic CO2 uptake, and increased electron transfer rate of PSI and PSII systems

The efficiency of atmospheric CO_2 uptake by plants and of its photosynthetic assimilation into organic compounds as the building blocks of biomass has major impact on wood production capacity. In accordance with the stomatal conductance data, all tetraploid plants analyzed showed significantly enhanced CO_2 assimilation rate as compared to diploid plants (Fig. 9). Net photosynthetic CO_2 uptake rates per unit leaf area has a positive linear relationship with the quantum yield of PSII or electron transfer rate (ETR) as shown by Kubota and Yoshimura (2002). Since the ETR is an estimate of the number of electrons passing through photosystems I and II, these associated parameters could be used for the prediction of photosynthetic capacity in leaves of different willow genotypes. Light saturation curves show increased rates of ETR(I) in tetraploid genotypes PP-E13 and PP-E6 under field conditions at higher light intensities (Fig. 10A). For PP-E13, ETR(II) was significantly greater, especially at photosynthetic photon flux density (PPFD) values of 450 μmol photons m^{-2} s^{-1} or above (Fig. 10B). ETR(I) and ETR(II)

.

values were generally lower in leaves of greenhouse-grown plants. Under these circumstances the photosynthetic capacities of tetraploid variants were found to be improved as indicated by both ETR(I) and ETR(II) values (Fig. 10 C and D).

In further characterization of photosynthetic functions of willow plants with different genome sizes, a set of chlorophyll fluorescence parameters were analyzed to provide quantitative information about the physiological functionality of these plants (Baker, 2008). The OJIP chlorophyll fluorescence transient reflects electron transport through redox components of PSII and PSI (Strasser et al., 2004). As indicated by the spider plot in Fig. 11, the tested genotypes showed clear differences in two fluorescence parameters: 1. Performance Index (PI) that describes the energy conservation between photons absorbed by PS II and the reduction of intersystem electron acceptors as well as the reduction of PSI end acceptors. Based on PI values, PP-E7, PP-E12 and PP-E13 plants exhibited the highest leaf photosynthetic activities. 2. Values dissipated energy flux per active reaction center (RC/ABS) were higher in leaves of some tetraploid lines (PP-E7, PP-E13, PP-E6).

Leaf chlorophyll (Chl) content is the key parameter for characterization of the physiological performance of plants including the determination of vegetation indices with woody species (Lu et al., 2015). Under greenhouse conditions, leaves of the tetraploid plants contained significantly greater concentrations of chlorophylls and carotenoids than the diploid plants (Table III). Elevated concentrations of these pigments were also detectable in field-grown leaves of the tetraploid variants relative to the diploid ones, but these differences did not reach the statistically significant levels.

Enlarged root system with alterations in anatomy and hormonal status as a consequence of autotetraploidization

Using the root phenotyping platform (Fig. 12A) growth of the root system was monitored by digital imaging from both side and bottom views. As shown by Fig. 12A the tetraploid PP-E12 plant developed an enlarged root system in comparison to the diploid plant. The differences are shown by images from both side and bottom views. Despite the fact that the cumulative white pixel counts generated cannot represent the whole root biomass, this approach could be used for

.

the detection of genotypic differences in root growth rate. During the first three weeks of root development, stem cuttings from tetraploid genotypes analyzed produced significantly higher root densities than cuttings from the diploid variant (Fig.12B, based on Welch's *t*-test). As the cultivation period proceeded, differences in root formation between tetraploid and diploid plants were increased considerably. In accordance with the data presented in Fig 12, the wet root weight data indicated that the autotetraploid willow plants produced larger root system than the diploid plants after seven weeks of growth (Fig. 13A). On the other hand, dry weight measurements showed that the differences between the genotypes were less pronounced which may be due to different water contents (Fig. 13B).

Analysis of cross-sections also revealed significant differences in anatomy between diploid and tetraploid roots. Root cortex cells were found to be larger in plants with duplicated genome size. (Fig. 14).

Together with the observed morphological and cellular differences, changes in hormonal pools were also detected between diploid and tetraploid roots. The root tips and the elongation zones were sampled separately for hormone analyses. Since characteristic differences were detected predominantly in root tip samples, hormone concentrations in this tissue (expressed as pmol per g fresh weight) are presented in Table IV. All tetraploid lines showed elevated contents of active cytokinins, with the most significant changes found in the root tips of PP-E7 and PP-E13 plants. These lines also exhibited high levels of cytokinin phosphates (i.e. cytokinin precursors). In the PP-E plants, trans-zeatin contents significantly exceeded the value of diploid plants. Cytokinin storage forms (cytokinin O-glucosides) were significantly elevated in PP-E7 and PP-E13 roots. Root tips from two tetraploid lines (PP-E7 and PP-E13) contained extremely high amounts of indole-3-acetic acid. Elevated concentrations of salicylic acid were characteristic for all three tetraploid variants. Only in PP-E7 plants GA_4 and GA_7 levels were enhanced.

DISCUSSION

Identification of energy willow variants with duplicated genome size

.

Speciation in the genus *Salix* has taken place in nature by intra- or inter-specific hybridizations that frequently resulted in allopolyploid progenies (Dorn 1976, Barcaccia et al., 2003). Breeding for improved biomass yield of the shrub willow is preferentially based on crossing programs also generating allopolyploid genotypes (Serapiglia et al., 2014). The present work provides a detailed characterization of autotetraploids to extend our knowledge about the morphological and developmental consequences of artificial genome duplication in this short rotation energy willow. Autotetraploid woody crops have been produced in several species including *Populus tremula* L. and *Populus pseudo-simonii*, (Ewald et al., 2009; Cai and Kang, 2011), *Paulownia tomentosa* (Tang et al., 2010), *Acacia dealbata* Link. and *Acacia mangium* Willd. (Blakesley, 2002); *Robinia pseudoacacia* (Ewald et al., 2009; Harbard et al., 2012; Wang et al., 2013), and *Betula platyphylla* (Mu et al., 2012). Colchicine, a microtubule polymerization inhibitor, has been used in a variety of methodologies involving treatment of seeds or apical meristems of germinated seedlings. *In vitro* cultured tissues with morphogenic potential can serve as ideal explants for the production of polyploid cells and regenerants (Tang et al., 2010; Cai and Kang, 2011).

In the case of willow variety Energo, our attempts to establish tissue cultures with shoot differentiation had failed, therefore the polyploidization protocol was optimized for the activation of axillary buds and the treatment of these organs with colchicine. One or two days after the removal of apical shoot meristems of willow plantlets grown *in vitro*, mitotic cells could be detected in cytological sections. Therefore this early developmental stage of axillary meristems was selected for treatment with the anaphase inhibitor. The outgrowing shoots could be cut off and further cultured for root formation. Plantlets from colchicine-treated buds showed a characteristic variation in leaf and root morphology already in *in vitro* cultures. The wider, round-shaped leaves and thicker roots could serve as early markers for polyploid nature (2n=4x=76) that was confirmed both by chromosome counting and flow cytometry (Fig. 1).

Exposure of multicellular organs such as axillary buds to colchicine is expected to produce mixoploid cell populations including unaffected diploid cells in addition to tetraploid ones. Therefore the outgrowing shoots may consist of diploid, chimeric or tetraploid tissues. This cellular heterogeneity necessitates continuous testing of the ploidy level of propagated plants both *in vitro* and in the field. These studies revealed that the majority of the lines were represented only by tetraploid plants and tetraploid shoots grew out from cuttings of these

.

genotypes. Two of the lines propagated through cuttings produced diploid and tetraploid clones. In these unstable lines diploid and tetraploid stems were recognized even on the same plant. This finding indicates that the observed variability of chromosome numbers can result from mixoploid nature or genome instability based on cellular events leading to different chromosomal compositions.

Autopolyploidy can alter primary and secondary growth in opposite ways

Growth characteristics, including biomass accumulation, could be followed by color (RGB) imaging of plants, which is one of the basic tools of plant phenotyping (Golzarian et al., 2011; Hartmann et al., 2011). Comparison of green surface area covered by green pixels, which can reflect shoot biomass revealed essential differences between the diploid line and tetraploid lines (Fig. 2A). This phenotypic parameter indicates higher or lower green biomass productivities for tetraploid plants as compared to the diploid ones. The genetic background of the observed variation in traits of genotypes with the same chromosome numbers is not known. Independent genome duplication events can generate different genomic structures in the tetraploid lines. Variation in several phenotypic characters of independent autotetraploid birch families was also observed after colchicine treatment of seeds of this tree species (Mu et al., 2012).

The above-ground biomass of an individual shoot is an integrative parameter therefore analysis of individual morphological traits is needed to provide a deeper insight into the developmental consequences of genome size alteration. Shoot height and stem diameter data clearly showed contrasting changes in willow plants after duplication of their genome (Fig. 2, B, C and Table I). Reduction in stem length or growth rate was reported for various autotetraploid tree species (Särkilahti and Valanne 1990; Griffin et al., 2015). Diploid *Paulownia tomentosa* plants were found to be by 10% taller than the tetraploids (Tang et al., 2010). Along with this trend, the mean height of the autotetraploid individuals of *Betula platyphylla* was by 19% lower than that of diploid birch plants (Mu et al., 2012). In the present greenhouse study analysis of independent tetraploid lines indicated considerable variation in stem height within the lines shown differences between the minimum and the maximum values as well as the extent of interquartile range (IQR)

.

(Fig. 2B). In agreement with other published examples (Tang et al., 2010; Mu et al., 2012), plants of several tetraploid willow lines (Fig. 2C and Table I) showed reduction in shoot height accompanied with wider stem formation as a consequence of autopolyploidization of willow plants. The tetraploid *Acacia mangium* trees developed significantly thicker bark of stem compared with diploid trees (Harbard et al., 2012). Data presented in Fig. 4 show that the most pronounced differences are found in the secondary xylem region that resulted in enlarged wood sections of the analyzed tetraploid willow plants. Divergent changes caused by artificial genome doubling in primary and secondary above-ground growth of woody species are unexpected features since these two functions correlate in nature as shown by studies on Mediterranean sub-shrubs species (Camarero et al., 2013). A similar synchrony between primary and secondary growth was also recorded over the growing season in boreal conifers (Huang et al., 2014). All these observations can indicate the existence of a regulatory mechanism coordinating parameters of organ growth that differs between diploid and autotetraploid plants of these tree species.

Apical meristems play a central role in the control of shoot growth. Presently basic information revealing the molecular or cellular basis of the reduced primary growth of autotetraploid tree stems is still missing. Comparison of the transcript profiles of tender shoot tips from diploid and tetraploid birch trees indicated several thousands of differentially expressed genes. Up-regulation of genes involved in biosynthesis or signal transduction of auxin and ethylene was detected in tetraploid shoot meristems (Mu et al., 2012). Genes of APETALA2/Ethylene Responsive Factor (AP2/ERF) domain-containing and AP2 domain class transcription factors were significantly activated in tetraploid meristems relative to diploids (Mu et al., 2012). As reviewed by Licausi et al., (2013), ectopic expression of selected AP2/ERF protein genes can result in growth retardation with simultaneous up-regulation of defense or stress-related genes. This hypothetic explanation of reduced growth of tetraploids needs experimental confirmation especially with consideration of the extremely large size and divergent roles of the AP2/ERF superfamily. Rao et al., (2015) predicted 173 AP2/ERF genes in the willow (*Salix arbutifolia*) genome.

The reduction of stem growth observed in the tetraploid willow plants is further supported by the 4.1-5.9 fold increase in active gibberellin (GA4 and GA7) content in tetraploid leaves as compared to diploid plants (Table II). In transgenic poplar (*P. tremula x P. alba*) plants, active

.

GA levels were increased by ectopic expression of the GA-Insensitive (GAI), or Repressor of GAI-Like (RGL) genes that caused variable degree of semi-dwarfism in these trees (Elia et al., 2012). An increase in the levels of various endogenous GAs was correlated with the extent of growth reduction. For example, the abundance of the inactive precursor GA_{20} in transgenic lines was increased 2.5-5.0-fold and the heights of field-grown transformants reached only 93-63% of the wild type plants. In contrast to the willow tetraploids, the shoot diameters of these transgenic poplar trees were also reduced. In another experimental system, hybrid poplar clones (*Populus tremula* x *Populus alba*) were transformed for RNAi down-regulation of C19 gibberellin 2-oxidase (GA2ox) genes (Guo et al., 2011). Suppression of *PtGA2ox4* and *PtGA2ox5* genes resulted in elevated GA_1 and GA_4 concentrations with simultaneous increase in leaf biomass and elongation of xylem fiber length and width in above-ground stems. In an earlier study, the *Arabidopsis* cDNA for GA 20-oxidase (*AtGA20ox1)* was overexpressed in hybrid aspen, *Populus tremula* L. × *P. tremuloides* Michx. (Eriksson et al., 2000). The transgenic plants produced high levels of 13-hydroxylated C19 GAs (GA_{20}, GA_1 and GA_8) and non-13-hydroxylated C19 GAs (GA_9, GA_4 and GA_{34}) in both internodes and leaves. Consequently these transgenic trees showed enhanced growth. The cited results from transgenic modification of GA metabolism in poplar can help explain certain characteristics of our autotetraploid willow genotypes. Considering the complexity of hormonal status modification in PP-E plants as shown in Table II, potential involvement of additional factors such as high concentrations of salicylic and jasmonic acids cannot be excluded from regulators of primary growth of these plants with duplicated genomes. As reviewed by Vicente and Plasencia (2011) in addition to its functions in biotic and abiotic stress responses, SA plays a crucial role in growth and development regulation in coordination with other plant hormones. The cross-talks between SA and GA can be relevant in the interpretation of the traits of polyploid willow plants. Alonso-Ramírez et al., (2009) showed that GAs were able to increase SA biosynthesis under stress conditions.

At present, only limited knowledge is available on the molecular or cellular mechanisms underlying enhanced secondary growth of autotetraploid tree stems that was observed here and in other studies (Särkilahti and Valanne 1990; Harbard et al., 2012; Mu et al., 2012; Griffin et al. 2015). In plants, three main types of meristematic tissues occur, namely shoot and root apical

.

meristems and procambium in vascular tissues. During wood formation vascular cambium activity and differentiation of secondary xylem from vascular cells are under a complex hormonal control (reviewed by Ye and Zhong, 2015). The vascular cambium is regulated by the two major plant hormones, auxin and cytokinins (Ruzicka et al., 2015). High expression of cytokinin biosynthetic genes as well as high endogenous levels of cytokinins were found in xylem precursor cells (Ohashi-Ito et al., 2014). Cytokinins are considered central regulators of cambial activity (Matsumoto-Kitano et al., 2008). This role of cytokinin is in accordance with enhanced active cytokinin levels and stimulation of wood development in tetraploid willow lines. Apart from cytokinins and auxins, gibberellins, ethylene and brassinosteroids are also involved in the control of xylem development (Didi et al., 2015). The pivotal role of gibberellins was shown by studies on transgenic poplar trees. RNAi suppression of two members (*PtGA2ox4* and *PtGA2ox5*) of the C19 gibberellin 2-oxidase (GA2ox) gene subfamily significantly increased the number of cells in the cambium zone (Guo et al., 2011). In leaves of these transgenic poplar plants both GA_1 and GA_4 levels were increased 1.4- and 1.9-fold, respectively, relative to control leaves. These transgenic plants developed wider stem diameters. The variety of transgenic approaches has been widely used for tree improvement (Dubouzet et al., 2013). The present production of tetraploid willow genotypes with extended secondary xylem tissues and wider stems in combination with improved photosynthesis, and enhanced root biomass can provide an example for the generation of novel genetic variation for improving traits of short rotation woody crops by non-transgenic means.

Duplication of the willow genome directs leaf functions towards improving biomass production

Comprehensive characterization of several independent autotetraploid lines of energy willow revealed substantial changes in leaf structure and functions as consequences of genome size modification. Increase of leaf biomass (Fig. 5D) is accompanied by alterations in leaf shape (Fig. 5A) and extended lamina length and width (Fig. 5, B and C). These characteristic phenotypic traits were also reported for other autotetraploid tree variants (Ewald et al., 2009; Cai and Kang 2011; Harbard et al., 2012; Mu et al., 2012). Cellular events beyond the ploidy-driven

.

enlargement of leaves are poorly understood in the case of tree species. Detailed analysis of diploid and autotetraploid cultivars of two grass species, *Lolium perenne* and *L. multiflorum* showed that the bigger leaf size of polyploids resulted mainly from the increased cell elongation rate, but not from the longer duration of the elongation period. The increased final cell size also contributed to organ size change (Sugiyama, 2005). A kinematic method showed no significant differences in cell division parameters, such as cell production rate and cell cycle duration between the diploid and tetraploid cultivars. In tetraploid willow leaves fewer but larger palisade parenchyma cells were detected (Fig. 7). These characteristics were also detected in autotetraploid *Pennisetum americanum* and *Medicago sativa* leaves where increased cell size, and fewer cells per unit leaf area were detected (see review by Warner and Edwards, 1993). Plant organ size is dependent on growth that is driven by cell division and expansion. Both of these processes are being regulated by phytohormones (Nelissen et al., 2012). In the division zone of maize leaves, i.e. in meristematic tissues, elevated concentrations of auxin (indole-3-acetic acid), and cytokinins (*trans*-zeatin and isopentenyladenine) were detected in comparison to mature or even senescing parts of leaves.

Exogenous cytokinin was reported to modulate the leaf shape (De Lojo et al., 2014). Peaks of gibberellins were found at the transition zone. Comparison of hormone contents of expanded diploid and tetraploid willow leaves provided characteristic indicators to explain size alterations. As shown by Table II, indole-3-acetic acid levels did not differ significantly between the analyzed genotypes. However, all tetraploid lines exhibited elevated level of the most physiologically active cytokinins including *trans*-zeatin. At the same time, enhanced cytokinin N-glucoside levels in tetraploids can be an indication for promoted deactivation of active cytokinins and thus their higher turn-over in tetraploid lines. The observed significant increase in GA_4 and GA_7 contents observed in tetraploid leaves can be considered as a potential factor in causing the enlargement of tetraploid willow leaves. This hypothesis is supported by studies on maize leaf development (Nelissen et al., 2012). Both the leaf elongation rate and the size of the division zone were increased in transgenic maize plants with elevated GA levels through the overproduction of the $AtGA_{20}$-oxidase1 enzyme. The GA-based interpretation of ploidy-induced alterations in willow leaf morphology is supported by studies on transgenic hybrid aspen overexpressing the GA_{20}-oxidase gene (Eriksson et al., 2000). The increased level of GAs in fully

.

expanded transgenic leaves caused the development of longer and broader leaves resulting in higher leaf fresh weights.

The experimental findings presented here indicate that enlargement of foliage size generated by autotetraploidy was accompanied with improvement of the photosynthetic productivity of tetraploid willow plants. Increases in both the stomatal conductance and the CO_2 assimilation rate can be a prerequisite for the potential improvement of biomass yield (Fig. 8 and 9). Similarly these parameters were reported to be superior for tetraploid black locust (*Robinia pseudoacacia* L.) even under salt stress (Wang et al., 2013). In earlier studies on the polyploids of *Atriplex confertifolia* photosynthetic rates per cell were highly correlated with ploidy level and with the activity of RuBPC (ribulose 1,5-bisphosphate carboxylase) per bundle sheath cell (Warner and Edwards, 1989). In other autotetraploid species (*Medicago sativa* L. and *Pennisetum americanum* L.) doubled cell volume was accompanied with lower cell number per unit leaf area, subsequently the higher ploidy levels did not result in a change in the rate of photosynthesis per leaf area (see review by Warner and Edwards (1993). A similar conclusion was drawn by studies on a natural allotetraploid *(Glycine dolichocarpa)* where the light-saturated electron transport rate per cell was higher in the tetraploids with reduced number of palisade cells (Coate et al., 2012).

In the present study, the improvement of photochemical reactions was recorded by monitoring the electron transfer rate (ETR) of photosystems, PSI and II. Light response curves of PSI and PSII revealed higher rates per unit leaf area in the tetraploid leaves analyzed from plants grown under both field and greenhouse conditions (Fig. 10). Differences between diploid and tetraploid genotypes in ETR values of PSII were in general larger in plants grown in the greenhouse. Higher ETR values were reported for the tetraploid Japanese honeysuckle (*Lonicera japonica* Thunb.) cultivar than for the diploid one. Reduction of ETR by drought was smaller in this genotype (Li et al., 2009).

From several chlorophyll a fluorescence OJIP fast kinetics parameters, especially the performance index (PI) and the energy flux/reaction centers (RC/ABS) indicated significant differences between genotypes. These indicators are mostly used for monitoring stress response also in tree species (Desotgiu et al., 2012). The higher energy conservation with the increased CO_2 assimilation rate can contribute to increase in biomass productivity in these autotetraploid plants. Higher (by 25-30%) chlorophyll (a+b) contents in greenhouse-grown leaves (Table III) .

can reflect more efficient light utilization. Smaller differences in the chlorophyll contents between diploid and tetraploid plants were detectable under field conditions. Elevated levels of GAs and *trans*-zeatin measured in the field in the tetraploid willow plants can influence the photosynthetic events especially chloroplast functions. Jiang et al., (2012) analyzed effects of the DELLA gai-1 mutation on chloroplast biogenesis and concluded that GAs indirectly promote chloroplast division through their impact on leaf mesophyll cell expansion. A close link between cytokinins and chloroplast differentiation has been reported repeatedly (see review by Cortleven and Schmülling, 2015). Analytical studies on hormone contents of willow leaves identified salicylic acid (SA) as being significantly elevated after polyploidization (Table II). SA can be involved in various steps of photosynthetic regulation (see review by Vicente and Plasencia, 2011). Treatment of *Brassica juncea* plants with low concentration (10^{-5} M) of SA resulted in higher net photosynthetic rate and carboxylation efficiency (Fariduddin et al., 2003).

Characteristic anatomical changes caused by autotetraploidy include the considerable increase in mid-rib size (Fig. 6). The structure of these major veins with their numerous xylem conduits may affect the water-transport capacity. Taneda and Terashima (2012) reported coordination in the development of the midrib xylem and the leaf-lamina area. In the case of tetraploid willow plants, these two traits were enlarged simultaneously. As shown in Table II, accumulation of abscisic acid in leaves was not influenced significantly by genome size alteration. Abscisic acid content seems to reflect predominantly the water relations in plants. Another stress hormone jasmonic acid (JA) and its derivate, jasmonate-isoleucine were detected in leaves of tetraploids at higher concentrations than in diploid leaves. Jasmonate-isoleucine is the active form of JA in plants functioning in defense against insects, microbial pathogens and abiotic stresses (Browse 2009).

The autotetraploid genome of energy willow plants regulates the development of enlarged root system

Results of the phenotypic characterization of autoploid tree species published have only been focused on the above-ground traits (Blakesley 2002; Ewald et al., 2009; Tang et al., 2010; Cai and Kang, 2011; Harbard et al., 2012; Mu et al., 2012). The present study extends this knowledge and shows substantial changes in the size and structure of roots developed by willow plants with

.

2n=4x=76 chromosomes relative to diploids. As an outcome of intensified plant phenotyping research, several alternative methods exist for the non-destructive imaging of root systems grown either in soil-free media or rhizotrons filled with soil (reviewed by Walter et al., 2015). Differences in root biomass between genotypes were recorded already during the first weeks (Fig. 12B). After a longer growing period, the tetraploid genotypes produced significantly larger root biomass. The functions of root meristems including stem cells are under the control of a complex hormonal network that regulates the growth of root system (see review by Pacifici et al., 2015). Accordingly the hormone data provided can support the interpretation of the increased root production in the tetraploid willow lines. Significant increases were detected in the levels of active cytokinins, indole-3-acetic acid, and salicylic acid in the root tips of the PP-E7 and the PP-E13 genotypes (Table IV). Lack of correlation was reported between concentrations of gibberellins and root biomass. The GA-deficient (35S:*PcGA2ox*1) and GA-insensitive (35S:*rgl1*) transgenic Populus plants developed larger root system regardless of lower or higher GA contents in the root tissues (Guo et al., 2010). In semi-dwarf hybrid poplar with elevated GAs, root biomass was enhanced (Elias et al., 2012). Plants with enlarged root system, carrying the tetraploid willow genotypes described can be more efficient in reaching and extracting nutrients and water even under conditions of limited availability. These plants can also be used for detoxification of contaminated soils. Both green and root biomass productivities determine the effectiveness of phytoremediation by trees species in removing heavy metals and organic contaminants from the environment (Marmiroli et al., 2011).

CONCLUSIONS

Artificial production of novel willow genotypes with autotetraploid genomes resulted in substantial modifications in the developmental program that can be valuable for wider use of this species as a short-rotation energy crop. The environmental impact of the increased CO_2 fixation and improved photosynthetic efficiency can attract special attention in attempts to reduce the negative impacts of climate changes. Despite the fact that the present work is focused on the early developmental phase of tetraploid willow plants, several of the described traits can play a role in wood productivity during the subsequent cultivation of these genotypes in the short rotation

.

system. Based on the observed morphological and physiological features of these new genotypes, the application of autopolyploidization as an old breeding technique with new potentials can gain increasing significance, especially in the improvement of vegetatively propagated woody species. Plants bred with this chromosome engineering technique are not considered as Genetically Modified Organisms (GMOs). This legal status opens large potentials even in countries or regions where breeding and cultivation of transgenic crops are prohibited by law. The data presented are consistent with several previously described characteristics of other autotetraploid woody plants where duplication of the plant genome caused very complex, multiple changes at the anatomical and morphological levels and in growth parameters of above-ground organs. Furthermore, this work provides additional information about alterations in the hormonal status of leaves and root tips as well as the stimulation of root development. We propose a key role for the increased gibberellin and cytokinin levels in controlling traits of autotetraploid woody plants. Importantly, the present interpretation of new tetraploid phenotypes could frequently be based on results from studies on transgenic wood species. The tetraploid variants described can also serve as crossing partners with diploids in order to produce triploid genotypes, which have been shown to be the most productive genetic background in willow wood production (Serapiglia et al., 2014).

MATERIALS AND METHODS

In vitro polyploidization of energy willow

Plantlets of 'Energo' variety kindly provided by Prof. Ferenc Kósa and Miklós Ift (Kreátor 2005 Kft, Budapest, Hungary) were propagated as *in vitro* sterile cultures with half strength concentration of hormone-free MS medium (Murashige and Skoog, 1962). These cultures were maintained under continuous light. Shoot apical meristems of 8-10 cm plantlets were decapitated and 48 hrs later stem sections with axillary buds were placed into sterile colchicine solution (0.05% or 0.1 % w/v) and incubated for 48 hrs in dark. After colchicine treatment, these stem sections were rinsed three times in sterile distilled water and placed on hormone-free 0.6% (w/v) agar medium without colchicine. Two-to-three centimeters long shoots grown from the treated

.

axillary buds were cut and placed in agar-solidified culture medium and used for further *in vitro* propagation. The differentiated roots were used for ploidy analyses. During the years, the tetraploid plantlets were maintained and propagated by nodal cuttings *in vitro* and 8-10 cm high, rooted plantlets were transferred to soil in the greenhouse. Under these conditions, these willow plants developed green woody stems that can be used as a propagation material for both greenhouse and field studies. Not all lines were available for each comparison, but all lines that were analyzed for a given comparison are shown in the corresponding figure.

Flow cytometry

Root tips (approximately 5-10 mm) of 2 weeks old cuttings were excised from the plants grown either in agar medium or in water used for rooting willow cuttings. Determination of ploidy levels was conducted with flow cytometry (BD FACSCalibur™) equipped with 532 nm green solid-state laser, operating at 30 mW. Nuclei extractions were done by chopping 15 mg of root tips on ice with a razor blade in a 55 mm Petri dish containing 1 ml Galbraith's buffer (Galbraith et al., 1983): 0.2 M Tris–HCl, 45 mM $MgCl_2$, 30 mM sodium citrate, 20 mM 4-morpholinepropane sulfonate, 1% (v/v) Triton X-100, pH 7.0) and then filtered through a 40-µm nylon mesh. The suspension of released nuclei was stained with 1 µg ml^{-1} of propidium iodide (PI, Sigma) for 10 min. At least 5000 gated particles were analyzed per sample. Identical instrument settings were used in order to have comparable relative fluorescence intensity values while analyzing diploid and tetraploid samples. For testing of uniformity of ploidy level, multiple stem cuttings were used for a given plant.

Chromosome counting

For the determination of chromosome numbers in mitotic willow cells, the previously described protocol developed for energy willow was used (Németh et al., 2013). Briefly, the mitotic events were synchronized by cold treatment at 4°C for 4 days. After 22 hrs incubation at room temperature, root tips were collected and fixed in Carnoy's solution (ethanol : acetic acid, 3:1 v/v). Cell walls of the fixed roots were digested in 1% enzyme mixture: 0.3% (w/v) cellulase, 0.3 % (w/v) pectolyase, 0.3% (w/v) cytohelicase and squash preparations were made in 45% acetic .

acid. Glass slides were exposed to liquid nitrogen and after removal of coverslips, cells were stained with 4',6-diamidino-2-phenylindole (DAPI) and observed with Olympus FV1000 confocal microscope.

Phenotyping of shoot and root growth

As members of the European Plant Phenotyping Network, we have constructed a semi-automatic platform that was previously used for phenotyping above-ground organs of barley and wheat plants (Cseri et al., 2013; Fehér-Juhász et al., 2014). Single dormant stem cuttings were planted into radio-tagged plexiglass columns with a mixture of 80 % Terra peat soil and 20 % sandy soil. Five plexiglass columns surrounded with PVC tube were placed on a metal rack. Three racks were used for each genotype with random arrangement. Only the shoot-forming cuttings and healthy shoots were included in the analyses. The racks were rearranged every week after each imaging during the experiments. The level of illumination in the greenhouse was ca. 400 µmol photons/m^2/s. This level was fairly constant during the whole illumination period. Watering and digital imaging were performed once a week. Shoots developed from dormant buds were photographed by an Olympus C-7070WZ digital camera from 7 different side positions, produced by 51.4° step rotation of the pot. Plant-related pixels were determined by separating the pot and background from the plant in each photograph by using an in-house developed image analysis software tool. The shoot and leaf surface that corresponds to the plant-related pixel number was provided as the average of green pixel counts derived from pictures of seven projections to minimize the variations in superposition of leaves and shoots.

In the case of roots, the plexiglass columns were photographed from 4 different side positions and from the bottom. The root-related white pixels were identified by subtracting the black soil background from the images. Pixel numbers were converted to millimeters using 65mm diameter pots captured in the images. To characterize the root area appearing at the surface of the chamber, the metric value of the area of the four side view projections (90° rotation) are summarized and the metric value of the area of the bottom view is added.

After completion of a seven-week phenotyping experiment, the rooted stems were removed from the soil and the roots were separated from the soils. Root weights were measured immediately

.

after removal from the soil (wet weight) or after air drying for 1 day at 21° C (dry weight) before weight determination.

For field analysis of early growth, we used second year shoots of plants from the stock collection that was established by planting willow plants grown in pots in the greenhouse in the soil of the experimental field in the spring (April). The unfertilized soil was cultivated by disc-harrow. Because of limitation in the available number of plants from different genotypes, these plants were placed in single rows with 1m apart. On average, 5-6 plants per genotype used in field analyses. Plant density was 50 cm within rows. After the growing season, one-year-old willow stems were cut off during the winter (January) to stimulate coppicing from the stools. The growth rate of newly developing shoots was measured to monitor both primary and secondary growth during an eight-day period at the end of April and the first days of May. During this period the average daily temperature was 21.5°C and average temperature at night was 9°C.

Leaf parenchyma and root cortex cell size determination

The youngest fully developed leaves were cut transversely at the middle of the leaf and fixed with 4% formaldehyde in PBS with 0.5 % Triton X-100 for 4 hrs at 23°C in a tube roller. After 3 x 10 mins washes, thin hand sections were prepared from the midpoint between the midrib and the border of leaves. Sections were mounted in 0.1 mg/ml calcofluor white in water and imaged using confocal laser scanning microscopy. Perimeters of leaf parenchyma cells were manually traced in Olympus Fluoview software and plotted. Using the same software, the number of cells in 100 µm was also calculated and plotted using Microsoft Excel software. For each genotype, four leaves were collected from two different plants and on more than 40 images a total of 200 cells were scored for cross-sectional area measurements. For root cortex cell size measurements, stem cuttings were rooted in water for 2 weeks. Root samples excised from the maturation zone were fixed, stained and imaged like in the case of leaf samples above. To eliminate the ambiguity of root cortex cell size at the boundary regions (close to epidermis and near stele regions), the middle 50% of the cortical region was identified as a curved strip using Olympus Fluoview software, and all cells in this region (including cells touching the strip borders) were manually traced to calculate the average cross-sectional area of the mid-cortex cells. For each genotype, four roots were collected from two different plants and on 12 non-consecutive hand sections a

.

minimum of 362 cells was scored for root mid-cortex region cell cross-sectional area measurements.

Microscopy of cells and tissue sections

Confocal laser scanning microscopy was performed using Olympus Fluoview FV1000 laser scanning confocal microscope (Olympus Life Science Europa GmbH, Hamburg, Germany). Microscope configuration was the following: objective lenses: UPLSAPO 10x (dry, NA: 0.4), UPLSAPO 20x (dry, NA: 0.75), UPLFLN 40x (oil, NA: 1.3); sampling speed: 4µs/pixel; line averaging: 2x; scanning mode: unidirectional; excitation: 405 nm (both for DAPI and calcofluor white); laser transmissivity: Less than 10%; main dichroic beamsplitter: DM405/488/543; intermediate dichroic beamsplitter: SDM 490; blue emission was detected between 425-475 nm. Bright field images were captured with the same laser line. For imaging hand-sectioned stem cross-sections, Olympus SZX12 stereo microscope with 0.5x and 1x objectives was used. For white light illumination, white LED light source (Photonic Optics, Vienna, Austria) in combination with transmission light mode was used. Photos of stem sections were captured using Olympus Camedia C7070 digital camera using DScaler software (version 4.1.15, www.dscaler.org). Composite images were prepared using CorelDraw Graphics Suite X7 (Corel Corporation, Ottawa, Canada).

Gas exchange measurements

Gas exchange parameters: CO_2 uptake rate, transpiration, and stomatal conductance were measured using a Licor 6400 gas analyzer (Licor, USA). Attached leaves of greenhouse-grown plants were inserted into the gas cuvette for the measurements. The gas cuvette conditions were set to 400 ppm CO_2, ambient temperature and growth light intensity of photosynthetic active radiation of 400-450 µmol m^{-2} s^{-1} (Mulkey and Smith, 1988; Taiz and Zeiger, 2010).

Electron transport rates (ETR): light response curves of PSI and PSII

The electron transport rates through PSII (ETR(II) = 0.5 * Y(II) * PPFD * 0.84), as well as through PSI (ETR(I) = 0.5 * Y(I) * PPFD * 0.84) were simultaneously measured using the

.

DUAL-PAM-100 system (WALZ, Effeltrich, Germany) (Baker, 2008, Klughammer and Schreiber, 1994). The effective quantum yield of photochemical energy conversion in PS II, Y(II)= (Fm' - F)/ Fm' (Genty et al., 1989), where Fo, Fo' are dark fluorescence yield from dark- and light-adapted leaf, respectively and Fm, Fm' are maximal fluorescence yield from dark- and light-adapted leaf, respectively was calculated. The photochemical the quantum yield of PSI, Y(I) is quantum yield of photochemical energy conversion. It is calculated as $Y(I) = (P_m' - P)/ P_m$ (Klughammer and Schreiber, 1994). The $P700^+$ signals (P) may vary between a minimal (P700 fully reduced) and a maximal level (P700 fully oxidized). The maximum level of $P700^+$ is called P_m in analogy with F_m. It was determined with application of a pulse (300 ms) of saturation light (10000 µE; 635 nm) after pre-illumination with far-red light. P_m' is analogous to the fluorescence parameter F_m' and was determined by applying saturation pulse on top of actinic illumination.

Chlorophyll a fluorescence fast kinetics measurements

OJIP chlorophyll a fluorescence transients were measured by a Plant Efficiency Analyzer (Pocket Pea, Hansatech, UK). The transients were induced by red light from an LED source (627 nm, up to 3500 µmol m^{-2} s^{-1} intensity). Prior to measurements, the adaxial surface of the selected leaves was adapted to darkness for 20 min using light-tight leaf-clips. The OJIP-test (Strasser et al., 2000) was used to analyze the chlorophyll a fluorescence transients and the following original data were acquired: O (Fo) initial fluorescence level (measured at 50 µs), P (Fm) maximal fluorescence intensity, as well as the J (at about 2 ms) and the I (at about 30 ms) intermediate fluorescence levels. From these specific fluorescence features the following parameters of photosynthetic efficiency were calculated: Maximal PSII quantum yield, F_v/F_m; The ratio of variable fluorescence to initial fluorescence, F_v/F_o where $F_v = F_m - F_o$; Probability of electron transport out of Q_A, $(1-V_j)/ V_j$ where $V_j = (F_{2ms} - F_o)/F_v$; Total complementary area between the fluorescence induction curve and F_m of the OJIP curve, Area; The amount of active reaction centers per absorption, RC/ABS (Zurek et al., 2014). Relative measurement of efficiency for electron transport, PI, Performance Index (Zivcak et al., 2008).

$$\mathbf{PI_{abs}} = \frac{\mathbf{1-(F_o/F_m)}}{\mathbf{M_o/V_j}} \times \frac{\mathbf{F_m - Fo}}{\mathbf{F_o}} \times \frac{\mathbf{1-V_j}}{\mathbf{V_j}}$$

.

Where $M_o = 4 * (F_{300\,\mu s} - F_o) / (F_M - Fo)$ represents the initial slope of fluorescence kinetics.

Chlorophyll and total carotenoid content estimation

Sampling was done on the 6th or 7th fully opened leaves from top. Pigment extraction was done using dimethylformamide (DMF) (Jacobsen et al., 2012). 0.8 cm leaf discs were immersed in 1 ml of DMF for 48 hours. The spectral determination of chlorophylls a and b, as well as total carotenoids was carried out according to Wellburn et al., 1994. Car(x+c) $\mu g/cm^2$ = total leaf carotenoids (xanthophyll(x)plus carotenes (c)).

Analysis of hormone contents in leaves and root tips

Leaf and root samples (50-100 mg fresh weight) were purified and analyzed according to Dobrev and Kaminek (2002) and Dobrev and Vankova (2012). Mixed samples of the youngest fully expanded leaves without the main vein or mixed samples of the root tips (c.a. 5 mm) or elongation zones (15-25mm from the tip) were homogenized with a ball mill (MM301, Retsch) and extracted in cold (-20 °C) methanol/water/formic acid (15/4/1 v/v/v). The following labeled internal standards (10 pmol/sample) were added: $^{13}C_6$-IAA (Cambridge Isotope Laboratories); $^{2}H_4$-SA (Sigma-Aldrich); $^{2}H_4$-SA (Sigma-Aldrich); and $^{2}H_3$-PA (phaseic acid) (NRC-PBI), $^{2}H_6$-ABA, $^{2}H_5$-transZ, $^{2}H_5$-transZR, $^{2}H_5$-transZ7G, $^{2}H_5$-transZ9G, $^{2}H_5$-transZOG, $^{2}H_5$-transZROG, $^{2}H_5$-transZRMP, $^{2}H_3$-DHZ, $^{2}H_3$-DHZR, $^{2}H_3$-DHZ9G, $^{2}H_6$-iP, $^{2}H_6$-iPR, $^{2}H_6$-iP7G, $^{2}H_6$- iP9G, $^{2}H_6$-iPRMP (Olchemim). The extract was purified using an SPE-C18 column (SepPak-C18, Waters) and a mixed mode reverse phase–cation exchange SPE column (Oasis-MCX, Waters). Two hormone fractions were sequentially eluted: (1) fraction A, eluted with methanol, containing auxins, ABA, SA, JA, GA; and (2) fraction B, eluted with 0.35 M NH_4OH in 60% methanol containing cytokinins. Hormone metabolites were analyzed using HPLC (Ultimate 3000, Dionex) coupled to a hybrid triple quadrupole/linear ion trap mass spectrometer (3200 Q TRAP, Applied Biosystems). Quantification of hormones was done using the isotope dilution method with multilevel calibration curves ($r^2 > 0.99$). Data processing was carried out with Analyst 1.5 software (Applied Biosystems). Data are presented as mean ± standard error.

.

Statistical analyses

For the statistical analyses, Welch's *t*-test was used for pairwise comparisons between the traits of diploid and tetraploid samples. Welch's *t*-test is an adaptation of Student's *t*-test and is more reliable if the samples have unequal sample sizes or variances (Ruxton 2006). Additionally, multiple comparison analyses were also performed using analysis of variance (ANOVA) followed by post hoc Tukey's honest significant difference (Tukey-HSD) test. Apart from Fig 2A, there were statistically significant differences between group means. Family-wise significance level for Tukey-HSD was set to a rather conservative value of 0.05 (Quinn and Keough, 2002), which granted an additional, more stringent level of significance threshold during comparison of tetraploids with diploids. Welch's *t*-test significance levels are indicated with asterisks which are underlined based on the results of Tukey-HSD test. In rare cases, P values calculated by Tukey's test fell into a higher significance interval as compared to P value obtained by *t*-test. These cases are indicated with an underlined period in the tables. For all statistical analyses, R statistical analysis software is used (developed by R Core Team, https://www.R-project.org/).

For all genotypes, the traits of individual plants were measured, and the distribution of data was displayed by box and whisker plots (Spitzer et al., 2014). The plots were generated with the webtool BoxPlotR (http://boxplot.tyers lab.com/) and edited with CorelDraw Graphics Suite X7. For phenotyping studies, the data analysis was performed by an in-house developed software package based on Matlab software tools (version 2008b) with the Image Processing Toolbox (The MathWorks Inc., Natick, MA, USA).

In photosynthetic studies the data were visualized and evaluated by the following methods: for ETR(I) and ETR(II) measurements Dual PAM version 1.18 and Origin 2015, for gas exchange measurements LI-6400 OPEN Software version 5.3 and Origin 2015**,** for chlorophyll fluorescence parameters deduced from OJIP fast kinetics measurements PEA Plus Version: 1.00 and Origin 2015**.** Spider graph values are displayed after normalization to respective value obtained in the diploid line.

ACKNOWLEDGMENTS

.

We thank F. Kósa and M. Ift (Kreátor Kft. Kaposvár, Hungary) for the initial stock of Energo willow cultivar, A. Herman for construction of the root phenotyping instrument in the GOP project, P. Ormos for providing greenhouse and field facilities, E. Kotogány for flow cytometric analyses and Zs. Kószó for technical contribution in microscopy.

AUTHOR CONTRIBUTIONS

D.D.: Conceived the project, wrote and revised the article with contributions from all the authors, K.T.: Production and multiplication of genotypes, A.Cs.: Phenotyping, K.P, I.V.: Photosynthetic measurements, A.V. N , B.N.: Colchicine treatments, chromosome counting, L.S.: Informatics, data analysis, Gy.F.: Tetrapolyploidization, R.V., P.D.: Hormone analysis, F.A.: Microscopy, statistical analyses and coordination of experiments.

TABLES

Table I. *Autotetraploidization generates opposite trends in alterations of the primary and the secondary growth of shoots emerged from dormant buds in the field.*

Geno-types	Shoot height (cm) Day 0	Shoot height (cm) Day 8	Primary growth (cm/8d)	Stem diameter (mm) Day 0	Stem diameter (mm) Day 8	Secondary growth in diameter (mm/8d)
Diploid	**52.02±3.79**	**83.08±7.04**	**31.07±4.24**	**5.76±0.77**	**6.59±0.60**	**0.82±0.21**
PP- E2	**42.68±2.39 *****	**68.36±4.57 *****	**25.68±0.99 *****	**6.31±0.41 ***	**7.27±0.71 ****	**0.96±0.35**
PP- E3	**39.48±3.64 *****	**64.96±5.61 *****	**25.48±1.47 *****	**6.33±0.66**	**7.59±0.68 *.**	**1.26±0.18 *****
PP- E4	**38.60±2.63 *****	**63.90±7.59 *****	**25.30±1.56 ****	**6.33±0.60 ***	**7.22±0.45 ***	**0.89±0.01**

.

PP- E5	**38.66±2.20 *****	**60.93±4.28 *****	**22.27±2.69 *****	**5.99±0.54**	**7.01±0.55**	**1.02±0.22**
PP- E6	**36.46±2.73 *****	**58.74±4.92 *****	**22.28±2.86 *****	**5.87±0.51**	**6.85±0.63**	**0.98±0.35**
PP- E7	**37.56±2.55 *****	**58.16±3.24 *****	**20.60±4.99 *****	**6.09±0.50**	**6.76±0.54**	**0.68±0.17**
PP- E12	**42.09±3.59 ** **	**69.76±4.36 ** **	**27.67±2.39 ** **	**5.90±0.53**	**7.46±0.64 ** **	**1.56±0.21 *****
PP- E13	**40.36±2.74 *****	**66.28±4.41 *****	**25.92±2.28 *****	**5.97±0.50**	**7.12±0.54 * **	**1.15±0.26 *****

The reduced shoot length at both recording times reflects a slower primary growth rate in early development of willow plants from the tetraploid variants. These plants developed wider stems and the growth rate of stem diameter was increased as a consequence of genome duplication. The number of measured shoots ranged 25-50 per genotype. Based on Welch's t-test, statistically significant events compared to diploids are indicated as *** P<0.01, ** P<0.05 and * P<0.1. Underlined asterisks indicate the level of significance based on post-hoc comparisons made with the Tukey's HSD test. Underlined period indicates that the P value obtained by Tukey's test falls into the next higher rank of significance as compared to significance level obtained by t-test. Based on Welch's *t*-test, statistically significant events compared to diploids are indicated as *** P<0.01, ** P<0.05 and * P<0.1. Underlined asterisks indicate the level of significance based on post-hoc comparisons made with the Tukey's HSD test. Underlined period indicates that the P value obtained by Tukey's test falls into the next higher rank of significance as compared to significance level obtained by *t*-test.

.

852 **Table II.** *Autotetraploidization caused essential changes in hormonal status of willow leaves*

Genotypes	Diploid	PP-E6	PP-E7	PP-E13
Active cytokinins	5.91±0.42	8.17±1.01 **	5.51±2.09	5.47±1.04
Trans-zeatin	0.67±0.31	2.48±1.48 **	0.79±0.13	0.72±0.25
Cytokinin phosphates	1.64±0.51	2.41±0.57	0.92±0.27	1.55±1.02
Cytokinin O-glucoside	25.71±2.40	25.67±2.43	20.66±3.57	18.27±3.45 **
Cytokinin N-glucosides	9.49±0.26	13.76±2.02 *.	10.94±0.68 *	14.52±1.54 **.
Abscisic acid	96.29±11.78	94.67±6.71	93.78±16.00	79.51±4.61
Indole-3-acetic acid	47.06±4.73	40.18±4.57	49.46±6.45	41.21±3.27
Salicylic acid	1288.85±87.31	2376.65±214.78 ***	2387.01±437.79 **	2520.09±586.93 *.
Jasmonic acid	6.92±0.51	9.16±1.37 *	14.10±4.05 *.	10.08±2.56
Jasmonate isoleucine	1.49±0.19	1.76±0.71	2.77±0.39 **	2.65±0.29 ***
Gibberellin GA_4	0.78±0.35	4.60±1.22 **.	3.20±1.03 **	3.23±0.98 **
Gibberellin GA_7	41.55±18.25	32.36±7.80	72.87±18.67 **	65.48±19.97 **

853

854 The values presented show the amounts of different hormones as pmol/g fresh weight. Mature
855 leaves from three plants were analyzed for each genotype. Based on Welch's *t*-test, statistically
856 significant events compared to diploids are indicated as *** P<0.01, ** P<0.05 and * P<0.1.
857 Underlined asterisks indicate the level of significance based on post-hoc comparisons made with

.

the Tukey's HSD test. Underlined period indicates that the P value obtained by Tukey's test falls into the next higher rank of significance as compared to significance level obtained by *t*-test.

Table III. ***L****eaf chlorophyll and total carotenoid contents of diploid and tetraploid plants grown under field and greenhouse conditions*

Sample	Chl a	Chl b	Chl (a+b)	Car (x+c)	Chl a	Chl b	Chl (a+b)	Car (x+c)
	(μg/cm^2)							
	Field grown plants				Greenhouse grown plants			
Diploid	**48.68 ±1.4**	**17.47 ±0.5**	**65.32 ±1.9**	**12.15 ±0.25**	**18.50 ±0.48**	**5.3 ±0.24**	**23.56 ±0.58**	**3.84 ±0.13**
PP-E6	**51.60 ±1.3**	**18.49 ±0.5**	**69.22 ±1.7**	**12.38 ±0.22**	**22.02 ±0.58 *****	**6.5 ±0.19 *****	**28.17 ±0.75 *****	**4.45 ±0.12 *****
PP-E7	**49.71 ±1.5**	**18.50 ±0.4**	**67.35 ±1.8**	**12.07 ±0.22**	**22.66 ±0.94 *****	**6.6 ±0.32 *****	**28.96 ±1.25 *****	**4.58 ±0.16 *****
PP-E13	**49.84 ±2.2**	**18.17 ±0.8**	**67.15 ±3.0**	**11.74 ±0.33**	**23.34 ±0.71 *****	**6.6 ±0.25 *****	**29.59 ±0.91 *****	**4.62 ±0.12 *****

Sampling was carried out from the 5th/ 6th fully developed young leaves (from top). Data are mean ± SE of six to seven independent plants per genotype. Based on Welch's *t*-test, statistically significant events compared to diploids are indicated as *** P<0.01, ** P<0.05 and * P<0.1. Underlined asterisks indicate the level of significance based on post-hoc comparisons made with the Tukey's HSD test.

.

871

872

873 **Table IV.** *Root tips from tetraploid plants differed from diploid plants in hormone contents*

Genotypes	Diploid	PP-E6	PP-E7	PP-E13
Active cytokinins	25.04±2.25	27.88±2.79	52.36±6.12 ***	40.68±3.96 ***
Trans-zeatin	1.37±1.04	2.71±0.92 ***	4.86±1.59 ***	2.88±0.32 ***
Cytokinin phosphates	17.92±2.20	20.08±2.13	33.97±2.58 ***	11.19±0.94 **
Cytokinin O-glucoside	2.09±0.72	2.18±0.83	11.90±0.78 ***	6.49±0.60 ***
Cytokinin N-glucoside	0.38±0.14	0.17±0.09	0.42±0.02	0.36±0.09
Abscisic acid	55.61±11.90	45.11±4.81	49.41±8.00	24.46±4.04 **.
Indole-3-acetic acid	234.16±10.28	197.91±21.35 *	890.72±96.54 ***	639.72±55.75 ***
Salicylic acid	184.75±23.28	308.82±18.20 ***	322.27±27.77 ***	241.44±30.48 *
Jasmonic acid	1150.00±189.18	1119.63±132.60	1072.51±101.23	834.16±37.72 *
Jasmonate isoleucine	148.65±48.20	120.19±16.44	157.46±20.39	118.99±17.86
Gibberellin GA_4	1.06±0.12	1.07±0.44	1.42±0.06	0.51±0.59

.

			**	
Gibberellin GA_7	**0.46±0.13**	**0.70±0.64**	**2.02±1.58 *.**	**1.17±0.59**

Stem cuttings were rooted in water for 2 weeks and 5-8 mm root tips were collected for hormone analysis. The values presented show the amounts of different hormones as pmol/g fresh weight. Roots from three plants were analyzed for each genotype. Based on Welch's *t*-test, statistically significant events compared to diploids are indicated as *** P<0.01, ** P<0.05 and * P<0.1. Underlined asterisks indicate the level of significance based on post-hoc comparisons made with the Tukey's HSD test. Underlined period indicates that the P value obtained by Tukey's test falls into the next higher rank of significance as compared to significance level obtained by t-test.

FIGURE LEGENDS

Figure 1. Identification of autotetraploid willow genotypes by chromosome counting (using DAPI stain) and flow cytometric analysis of relative DNA content (using propidium iodide). Shoots and plantlets emerged from colchicine-treated axillary buds were rooted and sampled as described in Materials and Methods. Representative data of at least three repetitions are shown. Scale bars: 5µm.

Figure 2. Variation in characteristics of shoot development in diploid and tetraploid genotypes of willow plants.

A, Comparison of green pixel-based shoot surface area monitored by digital photography to record above-ground biomass growth of willow plants from different genotypes in the greenhouse. Graph extension at the upper right shows interquartile ranges (25th and 75th percentiles) at week 7 for corresponding data points. Seventh week data points having the lowest (PP-E13) and highest (PP-E2) mean values are connected to the corresponding interquartile ranges with dashed lines. B, Box-plot presentation of average shoot lengths after 7 weeks of

.

growing period shows reduction in primary growth of autotetraploid plants in comparison to diploid plants. C, Box-plot presentation of average stem diameter after 7 weeks of growing period shows enhanced secondary growth of autotetraploid plants in comparison to diploid plants. Based on Welch's *t*-test, statistically significant events compared to diploids are indicated below the sample labels as *** P<0.01 and ** P<0.05. Underlined asterisks indicate the level of significance based on post-hoc comparisons made with the Tukey's honest significant difference (HSD) test. Box plot center lines show the medians; box limits indicate the 25th and 75th percentiles; whiskers extend 1.5 times the interquartile range from the 25th and 75th percentiles, outliers are represented by dots. Alternate boxes are shaded to differentiate neighboring boxes. n = 15, 15, 10, 11, 5, 15 sample points

Figure 3. Altered plant architecture and growth characteristics of autotetraploid willow plants grown under greenhouse conditions. Stem cuttings were planted into cultivation pots and the outgrowing shoots with characteristic phenotypic traits are presented. Note the development of larger, densely packed leaves of autotetraploid (PP-E7 and PP-E13) plants. Insets show thresholded binary images corresponding to the plants for a given view. Scale bar is 6.5 cm.

Figure 4. Wider stems with enlarged wood region in stem sections of tetraploid willow plants. Chart shows quantification of section areas representing bark, wood and pith regions (n=4). Statistically significant events (based on both Welch's *t*-test and Tukey's HSD post hoc test) compared to diploids are indicated for wood and bark regions as ***P<0.01. Dissection microscope images of a set of cross-sections are shown below the chart. Samples are collected at 120 cm from shoot tip of plants. Scale bar is 0.5 cm.

Figure 5. The autotetraploid genomic constitution of energy willow increases the foliage capacity of plants. A, Leaf morphology variations of willow plants grown in the field. B, Differences in leaf width between diploid and tetraploid willow plants grown in the greenhouse (n>52). C, Differences in lamina length between diploid and tetraploid willow plants grown in the greenhouse (n>37). D, Tetraploid willow plants produce more leaf biomass in comparison to diploid ones under greenhouse conditions (n>10). Based on Welch's *t*-tests, statistically

.

significant events compared to diploids are indicated below the sample labels as *** P<0.01, ** P<0.05 and * P<0.1. Underlined asterisks indicate the level of significance based on post-hoc comparisons made with the Tukey's HSD test. Boxplot center lines show the medians; box limits indicate the 25th and 75th percentiles; whiskers extend 1.5 times the interquartile range from the 25th and 75th percentiles, outliers are represented by dots.

Figure 6. Enhanced midrib-xylem development in leaves from tetraploid plants compared to diploid plant. Midrib cross-sectional areas were measured by manually tracing white colored midrib regions sampled from the mid-point of each leaf. Representative images of hand-sectioned material are shown. Scale bar 0.5 mm for all images. Boxplot center lines show the medians; box limits indicate the 25th and 75th percentiles; whiskers extend 1.5 times the interquartile range from the 25th and 75th percentiles (n=9). Statistically significant events (based on both Welch's *t*-test and Tukey's HSD post hoc test) compared to diploids are indicated below the sample labels as *** P<0.01.

Figure 7. Tetraploid willow plants have enlarged palisade parenchyma cells. A, Comparison of leaf cross-sections from diploid and tetraploid willow plants. Calcofluor white stained cell wall fluorescence (blue) was merged with transmission images. Arrows indicate palisade parenchyma layer of leaves. Scale bar is 20 µm for all images. B, Quantification of average palisade parenchyma cell size as cross-sectional area (n=200). C, Quantification of average number of parenchyma cells per 100µm-long distance (n=40). Boxplot center lines show the medians; box limits indicate the 25th and 75th percentiles; whiskers extend 1.5 times the interquartile range from the 25th and 75th percentiles, outliers are represented by dots. Statistically significant events (based on both Welch's *t*-test and Tukey's HSD post hoc test) compared to diploids are indicated below the sample labels as ***P<0.01 for both graphs.

Figure 8. Tetraploid willow plants transpire more water as shown by the elevated stomata conductance in leaves. Leaf stomatal conductance (g_s) measured on the 5th/ 6th fully developed younger leaves (from top) of willow plants. The measurements were recorded in air CO_2 concentration of 400 ppm, leaf temperature of 22°C, and PAR of 400- 430 µmol photons m^{-2} s^{-1}

.

(n=5). Boxplot center lines show the medians; box limits indicate the 25th and 75th percentiles; whiskers extend 1.5 times the interquartile range from the 25th and 75th percentiles, outliers are represented by dots. Based on Welch's *t*-test, statistically significant events compared to diploids are indicated below the sample labels as *** P<0.01 and ** P<0.05. Underlined asterisks indicate the level of significance based on post-hoc comparisons made with the Tukey's HSD test.

Figure 9. Autotetraploid willow plants absorb CO_2 more efficiently from the atmosphere. The rate of net CO_2 fixation was measured on the 5th/ 6th fully developed young leaves (from top) of willow plants at 400 – 430 µmol photons m^{-2} s^{-1} light intensity, 22°C temperature and 400 ppm ambient CO_2 level (n=5). Boxplot center lines show the medians; box limits indicate the 25th and 75th percentiles; whiskers extend 1.5 times the interquartile range from the 25th and 75th percentiles. Statistically significant events (based on both Welch's *t*-test and Tukey's HSD post hoc test) compared to diploids are indicated below the sample labels as ***P<0.01.

Figure 10. Improved photosynthetic capacity of tetraploid willow plants as indicated by electron transport rates (ETR) of photosystems I and II measured on leaf samples. Simultaneous light response curves of ETR(I) and ETR(II) were measured in the dark-adapted 5th/6th fully developed young leaves (from top) for both field and greenhouse genotypes by using DUAL PAM as described in Materials and Methods. A, ETR(I) under field conditions. B, ETR(II) under field conditions. Leaves of field-grown plants were collected in wet tissue, kept in ice box and ETR measurements were carried out within two hours of sample collection. C, ETR(I) under greenhouse conditions. D, ETR(II) under greenhouse conditions. Tetraploid willow genotypes are indicated as closed symbols and diploid genotype by open symbols. Data are mean ± SE of six independent plants per genotype. Based on Welch's *t*-test, statistically significant events (for the highest PPFD measurement) compared to diploids are indicated next to corresponding data points as *** P<0.01, ** P<0.05 and * P<0.01. Underlined asterisks indicate the level of significance based on post-hoc comparisons made with the Tukey's HSD test.

Figure 11. Spider plot of chlorophyll fluorescence parameters deduced from OJIP fast kinetics measurements. The figure shows the values of initial (F_o) and maximal (F_m) fluorescence levels; the F_v/F_m and the F_v/F_o (maximal PSII quantum yield) ratios, the $(1-V_j)/V_j$ parameter where $V_j = (F_{2ms} - F_o)/F_v$); the performance index (PI), the Area parameter, as well as the RC/ABS measured

.

on $5^{th}/6^{th}$ young fully developed leaves. The data are shown for the tetraploid lines (*open symbols*) after normalization to respective value obtained in the diploid line (*closed symbol*). Data are mean ± SE of six to seven independent greenhouse grown plants per genotype.

Figure 12. Significant stimulation of root development after duplication of genome size of energy willow. A, Side and bottom view of roots from the diploid and the tetraploid (PP-E12) plants grown in soil in transparent wall plexiglass columns. Digital images were taken at the third week of cultivation. Scale bar is 2 cm for all images. B, Total surface area (in mm^2) occupied by white pixels was used to monitor root biomass growth to compare diploid and tetraploid willow plants during the early development. Boxplot center lines show the medians; box limits indicate the 25th and 75th percentiles; whiskers extend 1.5 times the interquartile range from the 25th and 75th percentiles, outliers are represented by dots. Based on Welch's *t*-test, statistically significant events compared to diploids are indicated as **P<0.05 and *P<0.1. Underlined asterisks indicate the level of significance based on post-hoc comparisons made with the Tukey's HSD test. n = 10 sample points.

Figure 13. Autotetraploidization resulted in energy willow genotypes with increased root biomass. A, Experiment 1: Plants from tetraploid genotypes developed significantly more root than the control diploid ones based on fresh weight measurements (g/plant, n=10). B, Experiment 2: Increased root biomass of tetraploid willow genotypes as compared to diploid plants based on dry weight measurements (g/plant, n=10). Boxplot center lines show the medians; box limits indicate the 25th and 75th percentiles; whiskers extend 1.5 times the interquartile range from the 25th and 75th percentiles, outliers are represented by dots. Based on Welch's *t*-test, statistically significant events compared to diploids are indicated below the sample labels as *** P<0.01, ** P<0.05 and * P<0.12. Underlined asterisks indicate the level of significance based on post-hoc comparisons made with the Tukey's HSD test.

Figure 14. Differences in root anatomy detected between diploid and tetraploid willow plants. A, Calcofluor white stained, hand sectioned roots (from maturation zone) of diploid and tetraploid plants were imaged using confocal laser scanning microscope. Note the larger cortical cells of the

.

tetraploid samples. Scale bar is 50μm for all images. B, Cortical cells of diploid and tetraploid roots were manually traced on hand-sectioned material using Olympus Fluoview software and average cross-sectional area of cortical cells were calculated and plotted for diploid and tetraploid samples (n>362). Boxplot center lines show the medians; box limits indicate the 25th and 75th percentiles; whiskers extend 1.5 times the interquartile range from the 25th and 75th percentiles, outliers are represented by dots. Statistically significant events a(based on both Welch's *t*-test and Tukey's HSD post hoc test) compared to diploids are indicated below the sample labels as *** P<0.01.

LITERATURE CITED

Alonso-Ramírez A, Rodríguez D, Reyes D, Jiménez JA, Nicolás G, López-Climent M, Gómez-Cadenas A, Nicoás C. (2009) Evidence for a role of gibberellins in salicylic acid-modulated early plant responses to abiotic stress in Arabidopsis seeds. Plant Physiol **150:** 1335–1344

Baker NR (2008) Chlorophyll fluorescence: a probe of photosynthesis in vivo. Annu Rev Plant Biol **59:** 89–113

Barcaccia G, Meneghetti S, Albertini E, Triest L, Lucchin M (2003) Linkage mapping in tetraploid willows: segregation of molecular markers and estimation of linkage phases support an allotetraploid structure for *Salix alba x Salix fragilis* interspecific hybrids. Heredity **90(2):** 169–80

Blakesley DA, Allen A, Pellny TK, Robersts AV (2002) Natural and induced polyploidy in *Acacia dealbata* Link. and *Acacia mangium* Willd. Ann Bot **90:** 391–398

Browse J (2009) Jasmonate passes muster: A receptor and targets for the defense hormone. Annu Rev Plant Biol **60**: 183–205.

.

Cai X, Kang XY (2011) In vitro tetraploid induction from leaf explants of *Populus pseudo-simonii* Kitag. Plant Cell Rep **30**:1771–1778

Camarero JJ, Palacio S, G. Montserrat-Martı G (2013) Contrasting seasonal overlaps between primary and secondary growth are linked to wood anatomy in Mediterranean sub-shrubs. Plant Biol **15**: 798–807

Cseri A, Sass L, Törjék O, Pauk J, Vass I, Dudits D (2013) Monitoring drought responses of barley genotypes with semi-robotic phenotyping platform and association analysis between recorded traits and allelic variants of some stress genes. Australian Journal of Crop Science 7**:**1560–1570

Coate JE, Luciano AK, Seralathan V, Minchew KJ, Owens TG, Doyle JJ (2012) Anatomical, biochemical, and photosynthetic responses to recent allopolyploidy in Glycine dolichocarpa (Fabaceae). Am J Bot **99**:55-67.

Cortleven A, Schmülling T (2015) Regulation of chloroplast development and function by cytokinin. J Exp Bot. **66**:4999-5013

Cunniff J, Cerasuolo M (2011) Lighting the way to willow biomass production. J Sci Food Agric **91**: 1733–1736

De Lojo J, Di Benedetto A (2014) Biomass accumulation and leaf shape can be modulated by an exogenous spray of 6-benzylaminopurine in the ornamental foliage plant, *Monstera deliciosa* (Liebm.) J Horticultural Sciences, Biotechnology **89**: 136-140

Desotgiu R, Pollastrini M, Cascio C, Giacomo Gerosa G, Riccardo Marzuoli R, Bussotti F (2012) Chlorophyll *a* fluorescence analysis along a vertical gradient of the crown in a poplar (Oxford clone) subjected to ozone and water stress. Tree Physiol **32:** 976–986

.

Didi V, Jackson P, Hejatko J (2015) Hormonal regulation of secondary cell wall formation. J Exp Bot **66**: 5015-5027

Dobrev P, Kamínek M (2002) Fast and efficient separation of cytokinins from auxin and abscisic acid and their purification using mixed-mode solid-phase extraction. J of Chromatography *A* **950:** 21-29

Dobrev PI, Vanková R (2012) Quantification of abscisic acid, cytokinin, and auxin content in salt-stressed plant tissues. *Methods in Molecular Biology* **913**: 251-261

Dorn RD (1976) A synopsis of American Salix. Can J Bot **54:** 2769–2789

Dubouzet JG, Strabala TJ, Wagner A (2013) Potential transgenic routes to increase tree biomass. Plant Science **212:** 72– 101

Elias AA, Busov VB, Kosola KR, Ma C, Etherington E, Shevchenko O, Gandhi H, Pearce DW, Rood SB, Strauss SH (2012) Green revolution trees: semidwarfism transgenes modify gibberellins, promote root growth, enhance morphological diversity, and reduce competitiveness in hybrid Poplar. Plant Physiol **160:** 1130–1144

Eriksson ME, Israelsson M, Olsson O, Moritz T (2000) Increased gibberellin biosynthesis in transgenic trees promotes growth, biomass production and xylem fiber length. Nat Biotechnol **18:** 784–788

Ewald D, Ulrich K, Naujoks G, Schöder MB (2009) Induction of tetraploid poplar and black locust plants using colchicine: chloroplast number as an early marker for selecting polyploids in vitro. Plant Cell Tissue Organ Cult **99:** 353–357

Fariduddin Q, Hayat S, Ahmad A (2003) Salicylic acid influences net photosynthetic rate, carboxylation efficiency, nitrate reductase activity, and seed yield in *Brassica juncea*. Photosynthetica **41:** 281–284.

.

Fehér-Juhász E, Majer P, Sass L, Lantos Cs, Csiszár L, Turóczy Z, Mihály R, Mai A, Horváth GV, Vass I, Dudits D, Pauk J (2014) Phenotyping shows improved physiological traits and seed yield of transgenic wheat plants expressing the alfalfa aldose reductase under permanent drought stress. Acta Physiol Plant **36:** 663–673

Galbraith DW, Harkins KR, Maddox JM, Ayres NM, Sharma DP, Firoozabady E (1983) Rapid flow cytometric analysis of the cell cycle in intact plant tissues. Science **220:** 1049–1051

Genty B, Briantais JM, Baker NR (1989) The relationship between the quantum yield of photosynthetic electron transport and quenching of chlorophyll fluorescence. Biochim Biophys Acta **990:** 87–92

Golzarian MR, Frick RA, Rajendran K, Berger B, Roy S, Tester M, Lun DS (2011). Accurate inference of shoot biomass from high-throughput images of cereal plants. Plant Methods **7:** 2

Gou J, Strauss SH, Tsai CJ, Fang K, Chen Y, Jiang X, Busov VB (2010) Gibberellins regulate lateral root formation in Populus through interactions with auxin and other hormones. Plant Cell **22:** 623–639

Gou J, Ma C, Kadmiel M, Gai Y, Strauss S, Jiang X, Busov V (2011) Tissue specific expression of Populus C19 GA 2-oxidases differentially regulate above- and below-ground biomass growth through control of bioactive GA concentrations. New Phytol **192:** 626–639

Griffin AR, Chi NQ, Harbard JL, Son DH, Harwood CE, Price A, Vuong TD, Anthony Koutoulis A, Thinh HH (2015) Breeding polyploid varieties of tropical acacias: progress and prospects. Southern Forests 2015: *1–10*

.

Harbard JL, Griffin AR, Foster S, Brooker C, Kha LD, Koutoulis A (2012) Production of colchicine-induced autotetraploids as a basis for sterility breeding in *Acacia mangium* Willd. Forestry **85:** 3427–3436

Hartmann A, Czauderna T, Hoffmann R, Stein N, Schreiber F (2011) HTPheno: an image analysis pipeline for high-throughput plant phenotyping. BMC Bioinformatics **12:** 148

Huang JG, Deslauriers A, Rossi S (2014) Xylem formation can be modeled statistically as a function of primary growth and cambium activity. New Phytol **203:** 831–841

Jacobsen S-E, Rosenqvist E, Bendevis M, PrometheusWiki contributors (2012) Chlorophyll extraction with Dimethylformamide DMF. In: *PrometheusWiki.* http://prometheuswiki.publish.csiro.au/tikicitation.php?page=Chlorophyll%20extraction%20with%20Dimethylformamide%20DMF

Jiang X, Li H, Wang T, Peng C, Wang H, Wu H, Wang X (2012) Gibberellin indirectly promotes chloroplast biogenesis as a means to maintain the chloroplast population of expanded cells. Plant J **72:** 768–780

Karp A, Hanley SJ, Trybush SO, Macalpine W, Pei M, Shield I (2011) Genetic improvement of willow for bioenergy and biofuels. J Integr Plant Biol **53(2):** 151–165

Klughammer C, Schreiber U (1994) An improved method, using saturating light pulses, for the determination of photosystem I quantum yield via P700+-absorbance changes at 830 nm. Planta **192:** 261–268

Kubota HF, Yoshimura Y (2002) Estimation of photosynthetic activity from the electron transport rate of photosystem 2 in film-sealed leaf of sweet potato, *Ipomoea batatas* Lam. Photosynthetica **40:** 337–341

.

Li WD, Biswas DK, Xu H, Xu CQ, Wang XZ, Liu JK, Jiang GM (2009) Photosynthetic responses to chromosome doubling in relation to leaf anatomy in *Lonicera japonica* subjected to water stress. Funct Plant Biol **36:** 783–792

Licausi F, Masaru Ohme-Takagi MO, Perata P (2013) APETALA2/Ethylene Responsive Factor (AP2/ERF) transcription factors: mediators of stress responses and developmental programs. New Phytol **199:** 639–649

Lu S, Lu X, ZhaoW, Liu Y, Wang Z, Omasa K (2015) Comparing vegetation indices for remote chlorophyll measurement of white poplar and Chinese elm leaves with different adaxial and abaxial surfaces. PMID: 26034132, J Exp Bot doi:10.1093/jxb/erv270

Marmiroli M, Pietrini F, Maestri E, Zacchini M, Marmiroli N, Massacci A (2011) Growth, physiological and molecular traits in *Salicaceae* trees investigated for phytoremediation of heavy metals and organics. Tree Physiol **31:** 1319–1334

Matsumoto-Kitano M, Kusumoto T, Tarkowski P, Kinoshita-Tsujimura K, Vaclavikova K, Miyawaki K, Kakimoto T (2008) Cytokinins are central regulators of cambial activity. Proc Natl Acad Sci U S A **105**: 20027-20031

Mu HZ, Liu ZJ, Lin L, Li HY, Jiang J, Liu GF (2012) Transcriptomic analysis of phenotypic changes in birch (*Betula platyphylla*) autotetraploids. Int J Mol Sci **13:** 13012–13029

Mulkey SS, **Smith M** (1988) Measurement of photosynthesis by Infra Red Gas Analysis. In CT Lange ed., Bioinstrumentation, Publication of the American Biology Teachers Association, pp 79–84

Murashige T, Skoog F (1962) A revised medium for rapid growth and bio-assays with tobacco tissue cultures. Physiol Plant **15(3):** 473–497.

.

Nelissen H, Rymen B, Jikumaru Y, Demuynck K, Lijsebettens MV, Kamiya Y, Inze D, Beemster GTS (2012) A local maximum in gibberellin levels regulates maize leaf growth by spatial control of cell division. Curr Biol **22:** 1183–1187

Németh AV, Dudits D, Molnár-Láng M, Linc G (2013) Molecular cytogenetic characterisation of *Salix viminalis* L. using repetitive DNA sequences. J Appl Genet **54:** 265–269

Newsholme C (1992) Willows, the *Genus Salix*. Timber Press, Portland, Oregon, USA.

Ohashi-Ito K, Saegusa M, Iwamoto K, Oda Y, Katayama H, Kojima M, Sakakibara H, Fukuda H (2014) A bHLH Complex Activates Vascular Cell Division via Cytokinin Action in Root Apical Meristem. Current Biology **24**: 2053-2058

Pacifici E, Polverari L, Sabatini S (2015) Plant hormone cross-talk: the pivot of root growth. J Exp Bot **66:** 1113–1121

Quinn GP and Keough MJ (2002) Experimental Design and Data Analysis for Biologists, Cambridge Univeristy Press, Cambridge, p49.

Rao G, Sui J, Zeng Y, He C, Zhang J (2015) Genome-wide analysis of the AP2/ERF gene family in *Salix arbutifolia*. FEBS Open Bio **(5):** 132–137

Ruxton GD (2006). The unequal variance t-test is an underused alternative to Student's t-test and the Mann–Whitney U test. Behavioral Ecology 17: 688–690.

Ruzicka K, Ursache R, Hejatko J, Helariutta Y (2015) Xylem development - from the cradle to the grave. New Phytologist **207**: 519-535

Särkilahti E and Valanne T (1990) Induced polyploid in Betula. Silva Fennica 24:227-234

.

Serapiglia MJ, Gouker FE, Smar LB (2014) Early selection of novel triploid hybrids of shrub willow with improved biomass yield relative to diploids. BMC Plant Biol **14:** 74–86

Strasser RJ, Tsimilli-Michael M, Srivastava A (2004) Analysis of the fluorescence transient. In G.C. Papageorgiou and Govindjee, eds, Advances in Photosynthesis and Respiration Series. Chlorophyll Fluorescence: a Signature of Photosynthesis. Springer, Dordrecht, The Netherlands, pp 321–362

Spitzer M, Wildenhain J, Rappsilber J, Tyers M. (2014) BoxPlotR: a web tool for generation of box plots. Nat Methods. **11**:121-122

Strasser RJ, **Srivastava A, Tsimilli-Michael M** (2000) The fluorescence transient as a tool to characterize and screen photosynthetic samples. In Yunus M, Pathre UV, eds, Probing photosynthesis: Mechanisms regulation and adaptation. Taylor & Francis, New York, pp 443–480

Suda Y, Argus GV (1968) Chromosome numbers of some North American Salix. Brittonia **20:** 191–197

Sugiyama SI (2005) Polyploidy and cellular mechanisms changing leaf size: comparison of diploid and autotetraploid populations in two species of Lolium. Ann Bot **96:** 931–938

Tackenberg O (2007) A new method for non-destructive measurement of biomass, growth rates, vertical biomass distribution and dry matter content based on digital image analysis. Annals of Botany **99**:777-783

Taiz L, **Zeiger E** (2010) Plant Physiology, Fifth Edition. Sinauer Associates, Inc. Sunderland, MA, USA

.

Taneda H, Terashima I (2012) Co-ordinated development of the leaf midrib xylem with the lamina in *Nicotiana tabacum*. Ann Bot **110**: 35–45

Tang ZQ, Chen DL, Song ZJ, He YC, Cai DT (2010) In vitro induction and identification of tetraploid plants of *Paulownia tomentosa*. Plant Cell Tissue Organ Cult **102:** 213–220

Vicente MRS, Plasencia J (2011) Salicylic acid beyond defence: its role in plant growth and development. J Exp Bot **62:** 3321–3338

.

Walter A, Liebisch F, Hund A (2015) Plant phenotyping: from bean weighing to image analysis. Plant Methods **11:**14

Wang J, Shi L, Song S, Tian J, Kang X (2013) Tetraploid production through zygotic chromosome doubling in *Populus*. Silva Fennica vol. 47 no. 2 article id 932. 12 p. ISSN-L 0037-5330 | ISSN 2242-4075 (Online)

Wang Z, Wang M, Liu L, Meng F (2013) Physiological and proteomic responses of diploid and tetraploid black locust (*Robinia pseudoacacia* L.) subjected to salt stress. Int. J. Mol. Sci. **14:**20299-20325

Warner DA. Edwards GE (1989) Effects of polyploidy on photosynthetic rates, photosynthetic enzymes, contents of DNA, chlorophyll, and sizes and numbers of photosynthetic cells in the C4 dicot *Atriplex confertifolia*. Plant Physiol **91:** 1143–1151

Warner DA, **Edwards GE (**1993) Effects of polyploidy on photosynthesis. Photosynth Res. **35**: 135-47.

Wellburn AR (1994) The spectral determination of chlorophylls *a* and *b*, as well as total carotenoids, using various solvents with spectrophotometers of different resolution. Journal of Plant Physiology **144**: 307-313.

.

Ye ZH, Zhong R (2015) Molecular control of wood formation in trees. Journal of Experimental Botany **66:** 4119–4131

Zivcak M, **Brestic M, Olsovska K, Slamka P** (2008) Performance index as a sensitive indicator of water stress in *Triticum aestivum* L. Plant Soil Environ **54(4):** 133–139

Zurek G, **Rybka K, Pogrzeba M, Krzyzak J, Prokopiuk K** (2014) Chlorophyll *a* fluorescence in evaluation of the effect of heavy metal soil contamination on perennial grasses. PLoS One 9:e91475. doi:10.1371/journal.pone.0091475

.

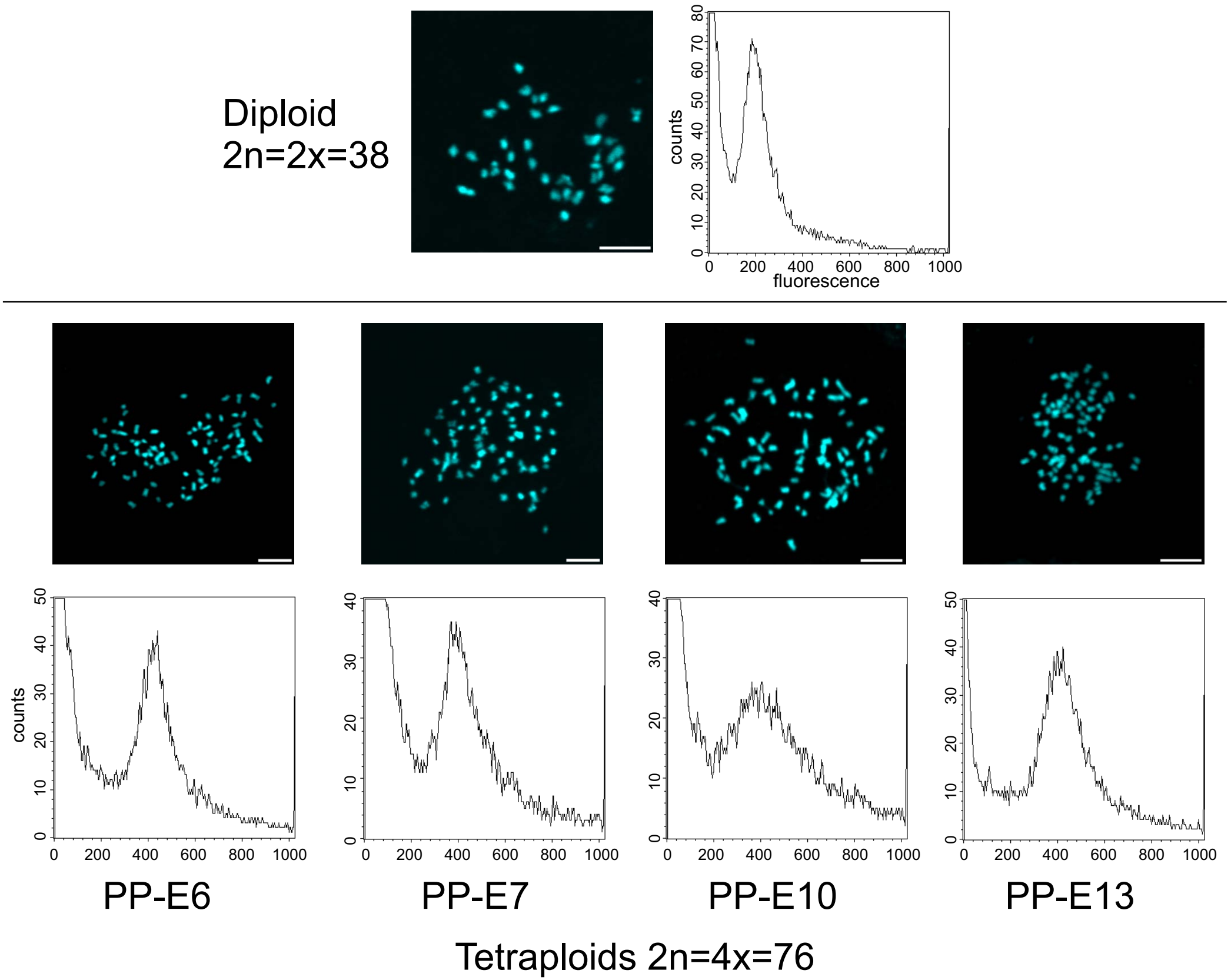

Figure 1. Identification of autotetraploid willow genotypes by chromosome counting (using DAPI stain) and flow cytometric analysis of relative DNA content (using propidium iodide). Shoots and plantlets emerged from colchicine-treated axillary buds were rooted and sampled as described in Materials and Methods. Representative data of at least three repetitions are shown. Scale bars: 5μm.

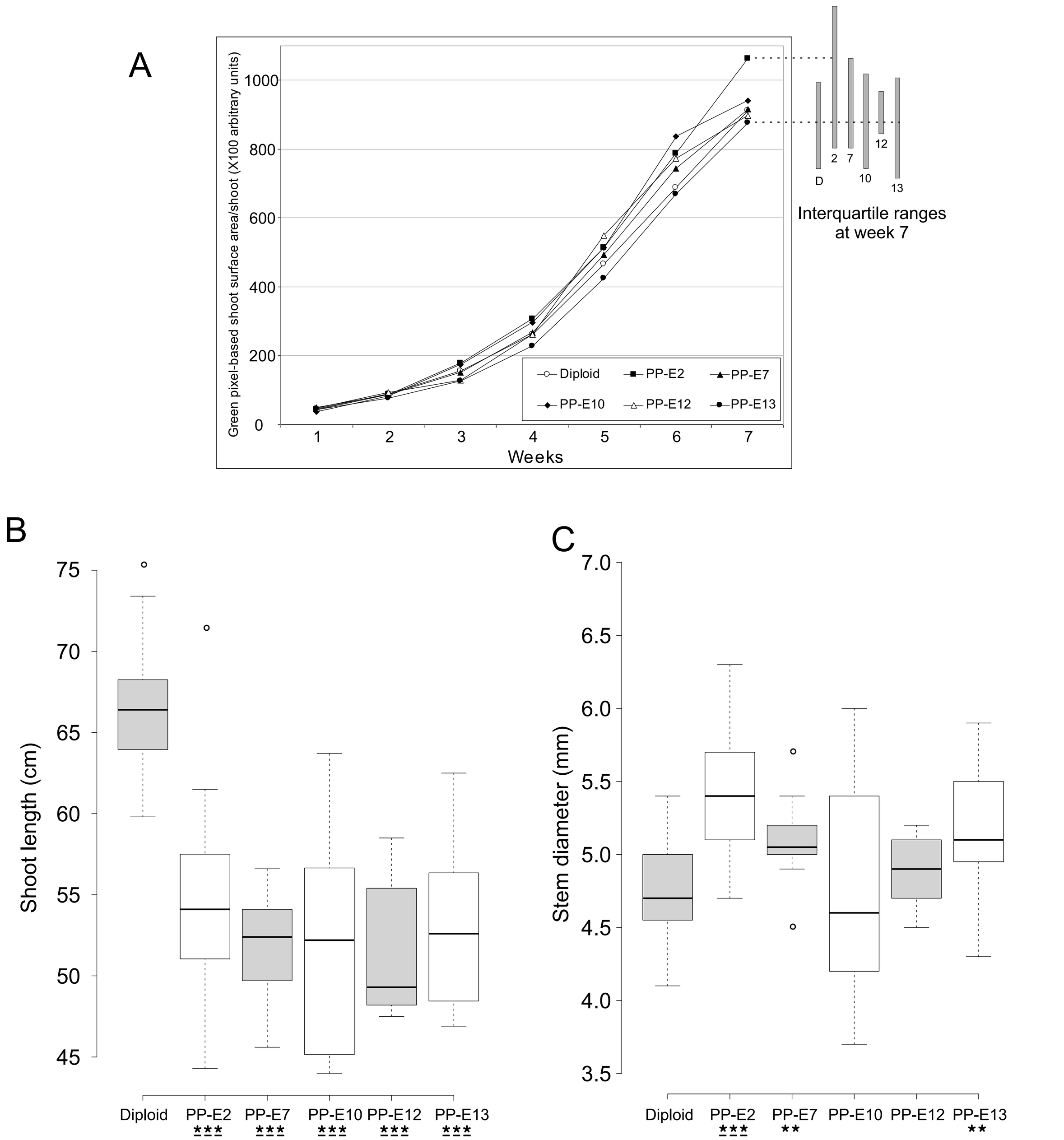

Figure 2. Variation in characteristics of shoot development in diploid and tetraploid genotypes of willow plants. A, Comparison of green pixel-based shoot surface area monitored by digital photography to record above-ground biomass growth of willow plants from different genotypes in the greenhouse. Graph extension at the upper right shows interquartile ranges (25th and 75th percentiles) at week 7 for corresponding data points. Seventh week data points having the lowest (PP-E13) and highest (PP-E2) mean values are connected to the corresponding interquartile ranges with dashed lines. B, Box-plot presentation of average shoot lengths after 7 weeks of growing period shows reduction in primary growth of autotetraploid plants in comparison to diploid plants. C, Box-plot presentation of average stem diameter after 7 weeks of growing period shows enhanced secondary growth of autotetraploid plants in comparison to diploid plants. Based on Welch's *t*-test, statistically significant events compared to diploids are indicated below the sample labels as *** P<0.01 and ** P<0.05. Underlined asterisks indicate the level of significance based on post-hoc comparisons made with the Tukey's honest significant difference (HSD) test. Box plot center lines show the medians; box limits indicate the 25th and 75th percentiles; whiskers extend 1.5 times the interquartile range from the 25th and 75th percentiles, outliers are represented by dots. Alternate boxes are shaded to differentiate neighboring boxes. n = 15, 15, 10, 11, 5, 15 sample points.

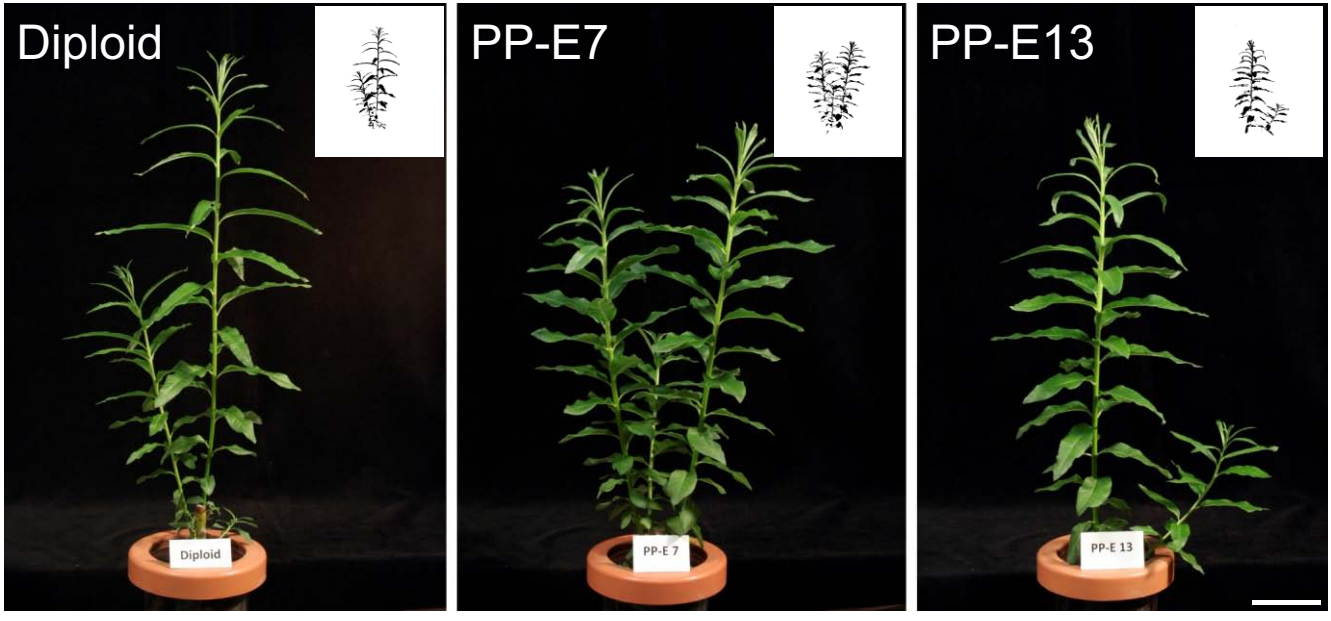

Figure 3. Altered plant architecture and growth characteristics of autotetraploid willow plants grown under greenhouse conditions. Stem cuttings were planted into cultivation pots and the outgrowing shoots with characteristic phenotypic traits are presented. Note the development of larger, densely packed leaves of autotetraploid (PP-E7 and PP-E13) plants. Insets show thresholded binary images corresponding to the plants for a given view. Scale bar is 6.5 cm.

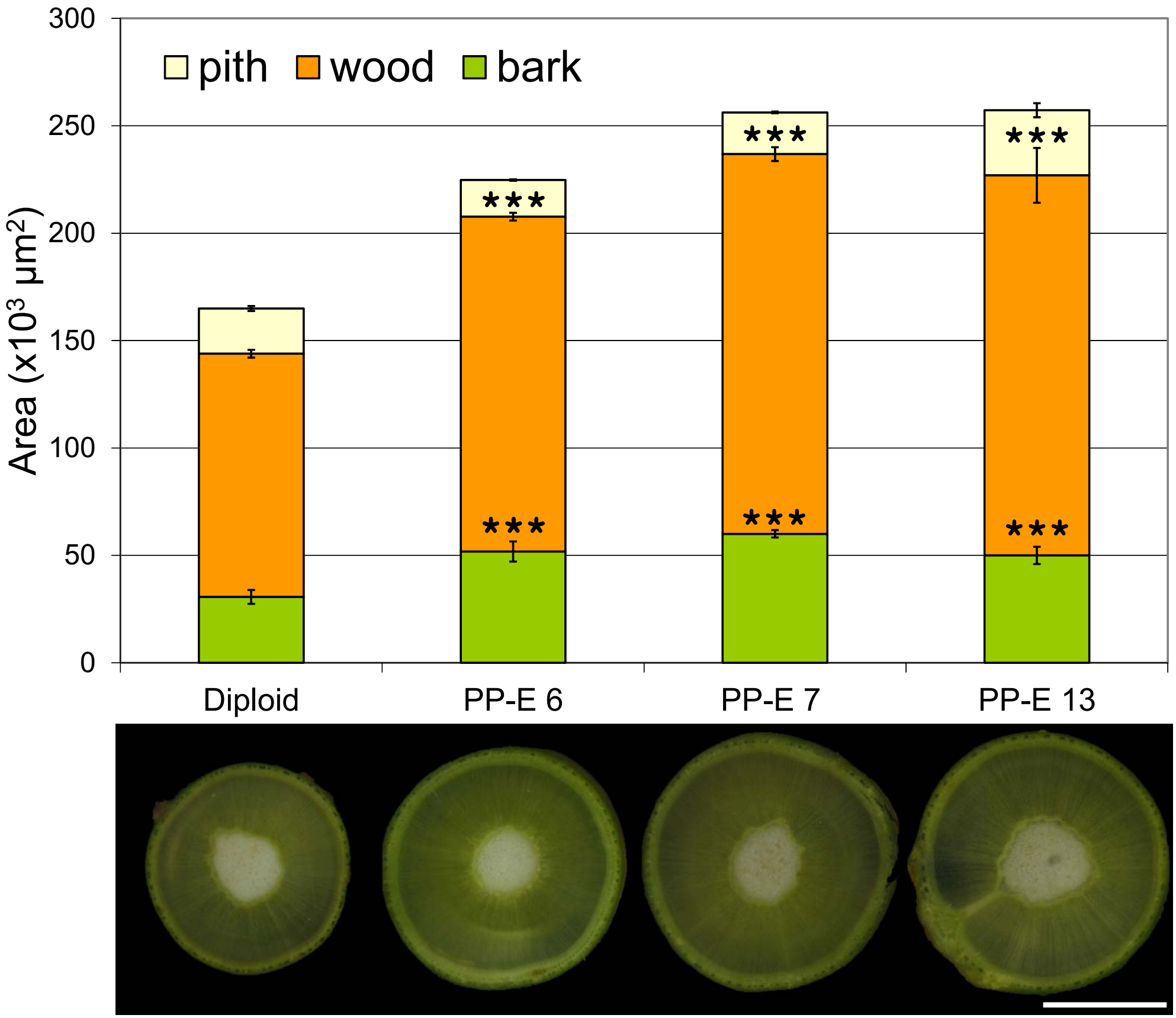

Figure 4. Wider stems with enlarged wood region in stem sections of tetraploid willow plants. Chart shows quantification of section areas representing bark, wood and pith regions (n=4). Statistically significant events (based on both Welch's *t*-test and Tukey's HSD post hoc test) compared to diploids are indicated for wood and bark regions as ***P<0.01. Dissection microscope images of a set of cross-sections are shown below the chart. Samples are collected at 120 cm from shoot tip of plants. Scale bar is 0.5 cm.

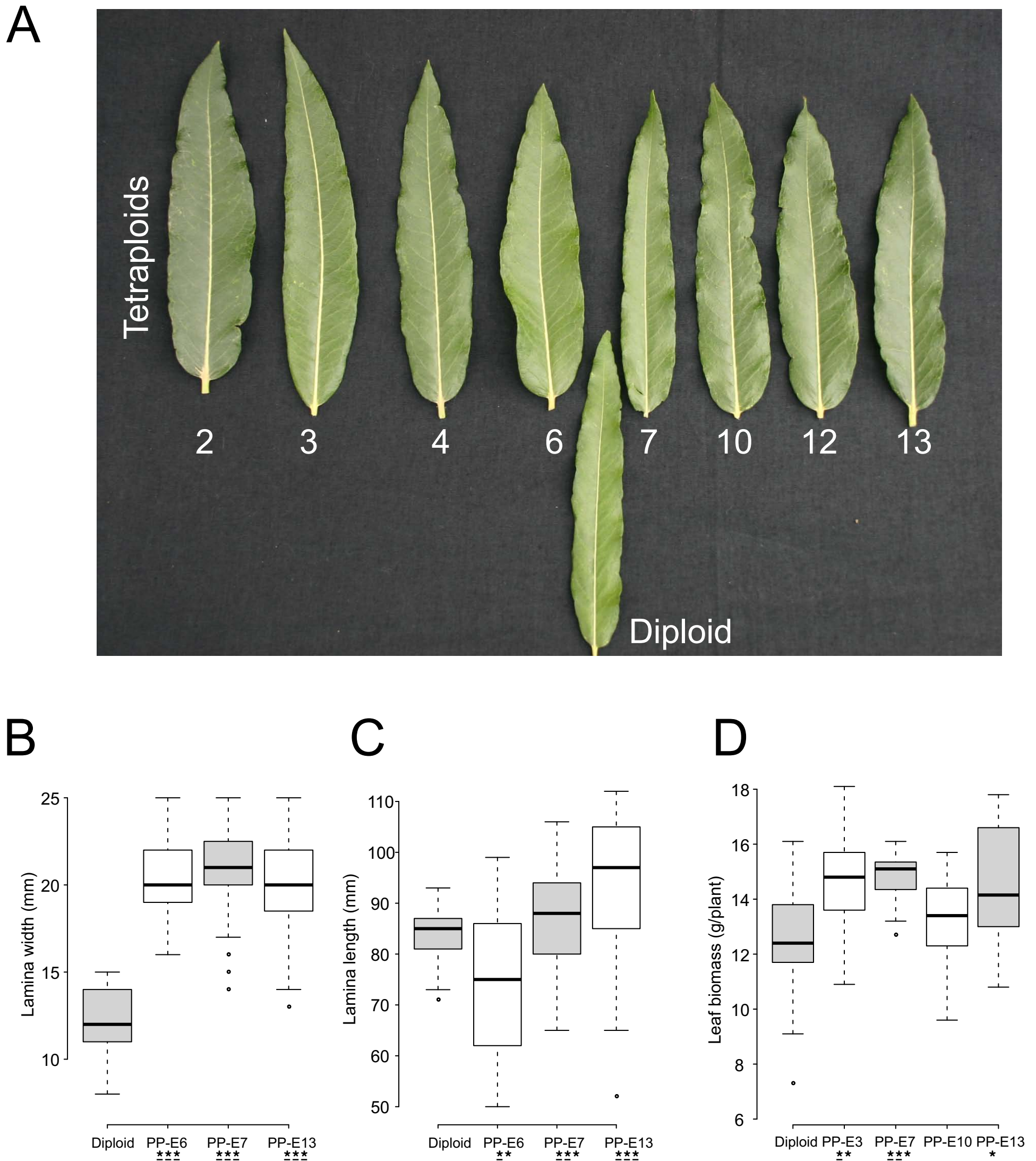

Figure 5. The autotetraploid genomic constitution of energy willow increases the foliage capacity of plants. A, Leaf morphology variations of willow plants grown in the field. B, Differences in leaf width between diploid and tetraploid willow plants grown in the greenhouse (n>52). C, Differences in lamina length between diploid and tetraploid willow plants grown in the greenhouse (n>37). D, Tetraploid willow plants produce more leaf biomass in comparison to diploid ones under greenhouse conditions (n>10). Based on Welch's *t*-tests, statistically significant events compared to diploids are indicated below the sample labels as *** P<0.01, ** P<0.05 and * P<0.1. Underlined asterisks indicate the level of significance based on post-hoc comparisons made with the Tukey's HSD test. Boxplot center lines show the medians; box limits indicate the 25th and 75th percentiles; whiskers extend 1.5 times the interquartile range from the 25th and 75th percentiles, outliers are represented by dots.

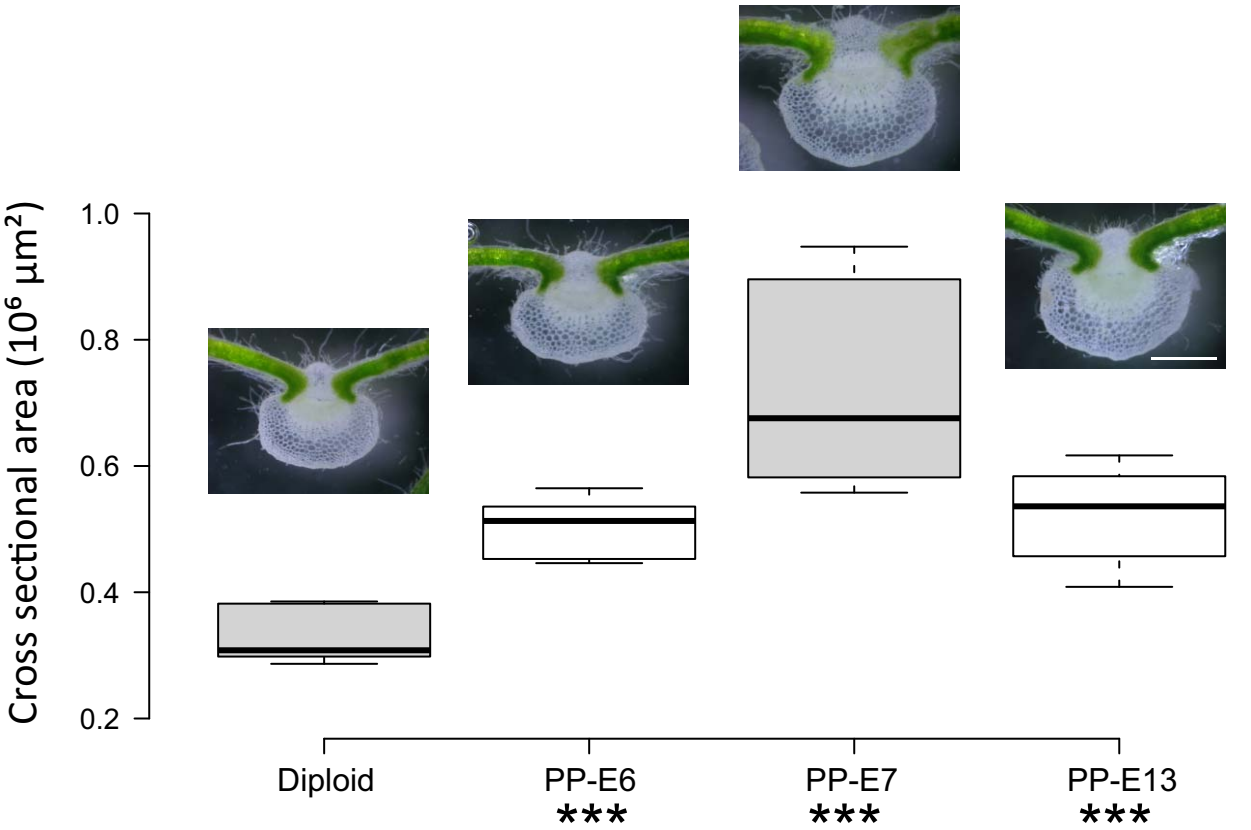

Figure 6. Enhanced midrib-xylem development in leaves from tetraploid plants compared to diploid plant. Midrib cross sectional areas were measured by manually tracing white colored midrib regions sampled from the mid-point of each leaf. Representative images of hand-sectioned material are shown on bar chart. Scale bar 0.5 mm. Boxplot center lines show the medians; box limits indicate the 25th and 75th percentiles; whiskers extend 1.5 times the interquartile range from the 25th and 75th percentiles (n=9). Statistically significant events (based on both Welch's *t*-test and Tukey's HSD post hoc test) compared to diploids are indicated below the sample labels as *** P<0.01.

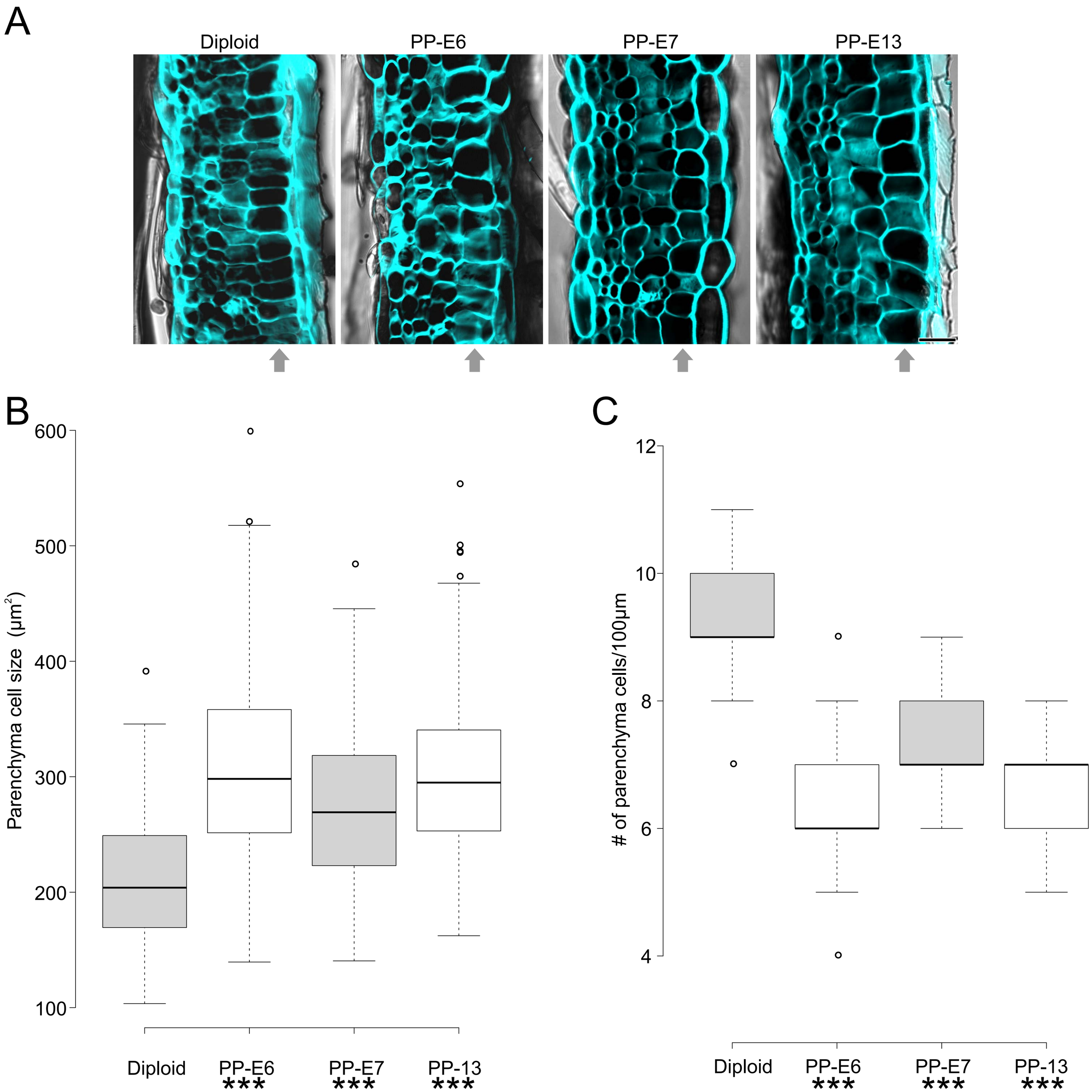

Figure 7. Tetraploid willow plants have enlarged palisade parenchyma cells. A, Comparison of leaf cross-sections from diploid and tetraploid willow plants. Calcofluor white stained cell wall fluorescence (blue) was merged with transmission images. Arrows indicate palisade parenchyma layer of leaves. Scale bar is 20 μm for all images. B, Quantification of average palisade parenchyma cell size as cross-sectional area (n=200). C, Quantification of average number of parenchyma cells per 100μm-long distance (n=40). Boxplot center lines show the medians; box limits indicate the 25th and 75th percentiles; whiskers extend 1.5 times the interquartile range from the 25th and 75th percentiles, outliers are represented by dots. Statistically significant events (based on both Welch's *t*-test and Tukey's HSD post hoc test) compared to diploids are indicated below the sample labels as ***P<0.01 for both graphs.

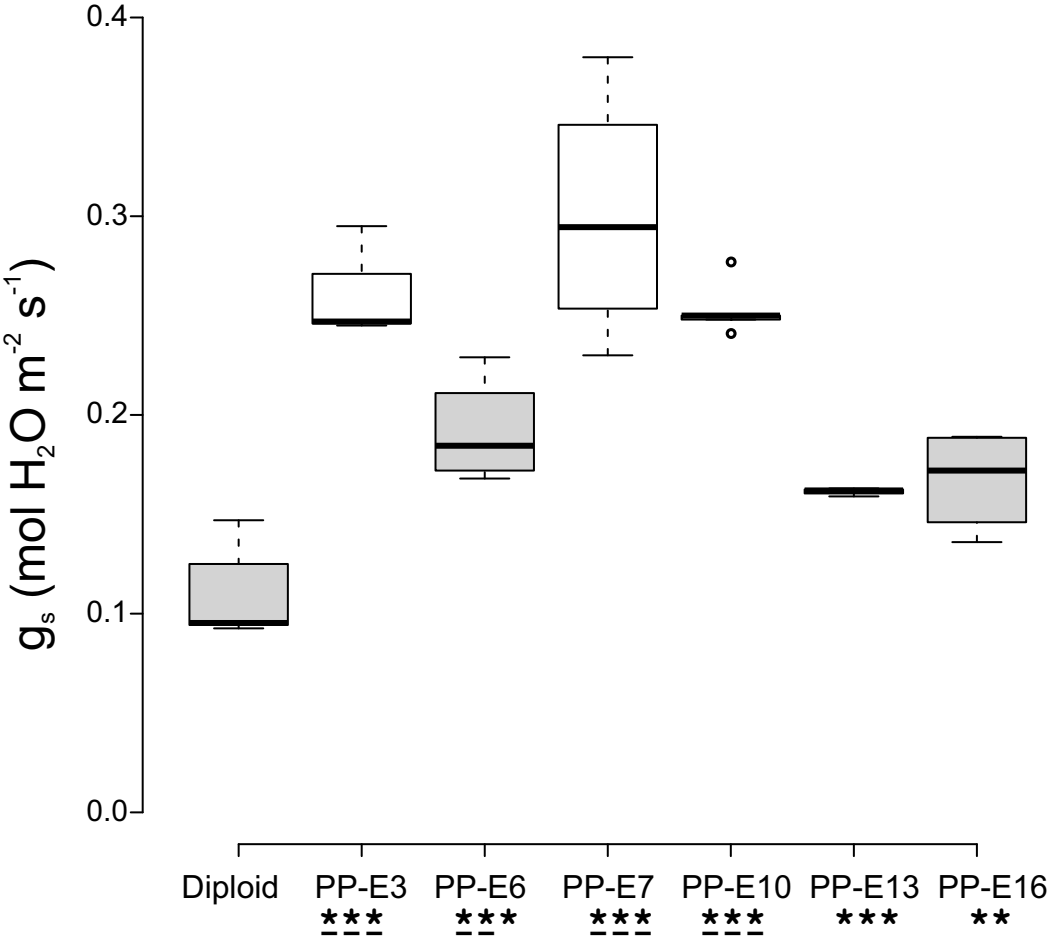

Figure 8. Tetraploid willow plants transpire more water as shown by the elevated stomata conductance in leaves. Leaf stomatal conductance (*g*s) measured on the 5th/ 6th fully developed younger leaves (*from top*) of willow plants. The measurements were recorded in air CO_2 concentration of 400 ppm, leaf temperature of 22°C, and PAR of 400-430 µmol photons m^{-2} s^{-1} (n=5). Boxplot center lines show the medians; box limits indicate the 25th and 75th percentiles; whiskers extend 1.5 times the interquartile range from the 25th and 75th percentiles, outliers are represented by dots. Based on Welch's *t*-test, statistically significant events compared to diploids are indicated below the sample labels as *** P<0.01 and ** P<0.05. Underlined asterisks indicate the level of significance based on post-hoc comparisons made with the Tukey's HSD test.

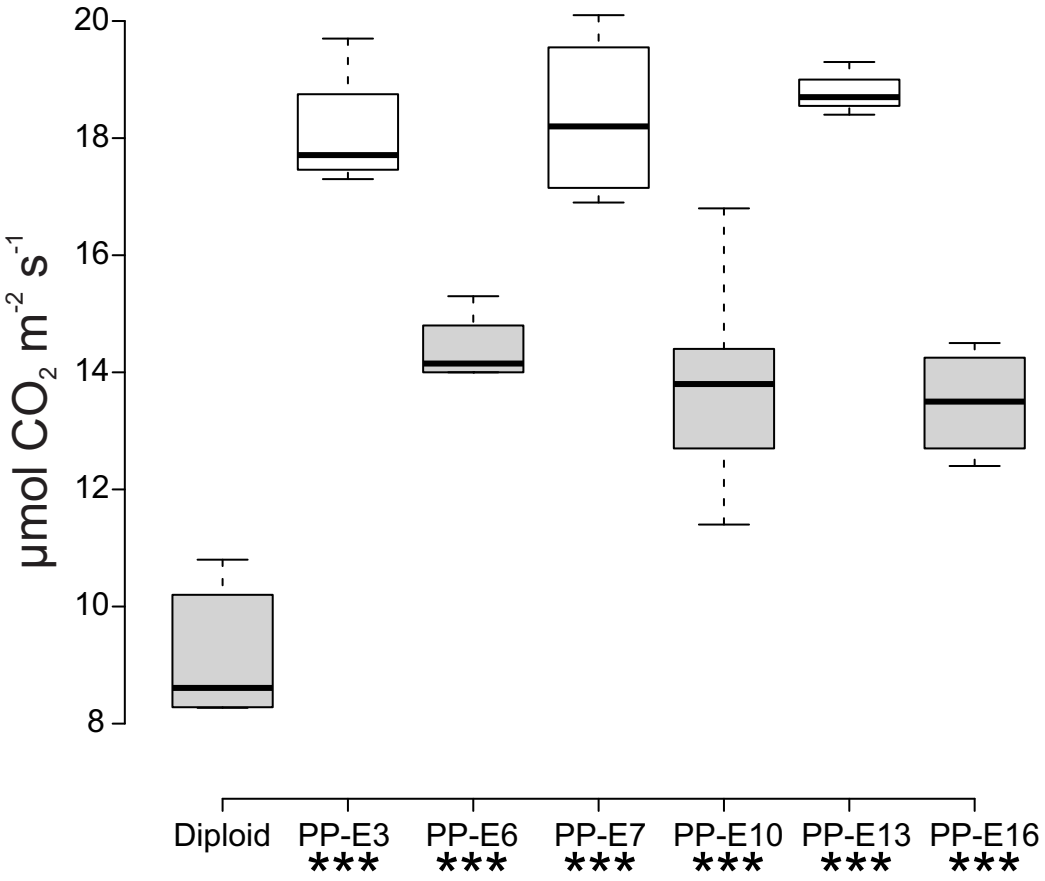

Figure 9. Autotetraploid willow plants absorb CO_2 more efficiently from the atmosphere. The rate of net CO_2 fixation was measured on the 5th/ 6th fully developed young leaves (*from top*) of willow plants at 400 - 430µmol photons m^{-2} s^{-1} light intensity, 22°C temperature and 400 ppm ambient CO_2 level (n=5). Boxplot center lines show the medians; box limits indicate the 25th and 75th percentiles; whiskers extend 1.5 times the interquartile range from the 25th and 75th percentiles. Statistically significant events (based on both Welch's *t*-test and Tukey's HSD post hoc test) compared to diploids are indicated below the sample labels as ***P<0.01.

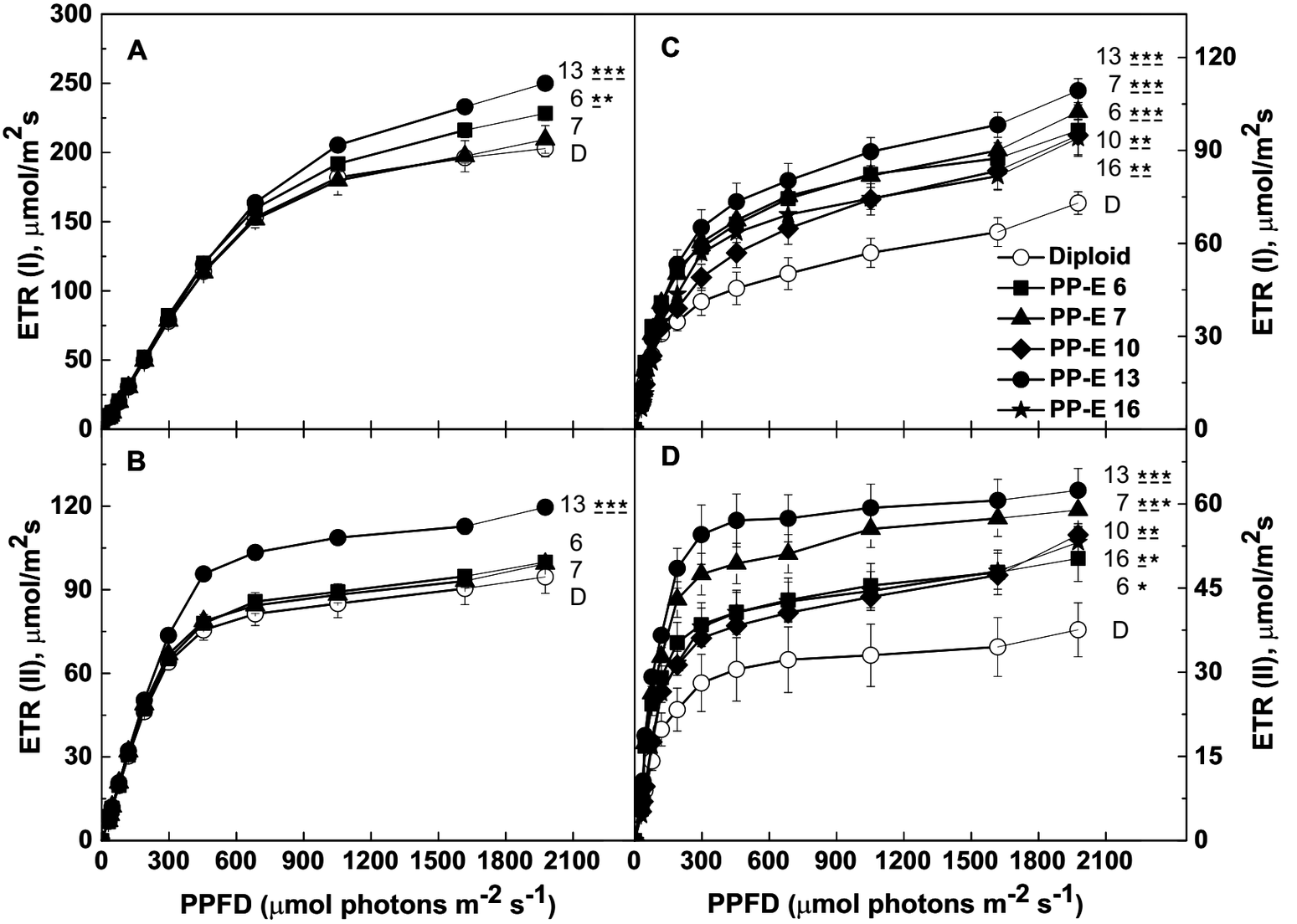

Figure 10. Improved photosynthetic capacity of tetraploid willow plants as indicated by electron transport rates (ETR) of photosystems I and II measured on leaf samples. Simultaneous light response curves of ETR(I) and ETR(II) were measured in the dark adapted 5th / 6th fully developed young leaves (*from top*) for both field and greenhouse genotypes by using DUAL PAM as described in Materials and Methods. **A,** ETR(I) under field conditions. **B,** ETR(II) under field conditions. Leaves of field-grown plants were collected in wet tissue, kept in ice box and ETR measurements were carried out within two hours of sample collection. **C,** ETR(I) under greenhouse conditions. **D,** ETR(II) under greenhouse conditions. Tetraploid willow genotypes are indicated as closed symbols and diploid genotype by open symbols. Data are mean ± SE of six independent plants per genotype. Based on Welch's *t*-test, statistically significant events (for the highest PPFD measurement) compared to diploids are indicated next to corresponding data points as *** P<0.01, ** P<0.05 and * P<0.01. Underlined asterisks indicate the level of significance based on post-hoc comparisons made with the Tukey's HSD test.

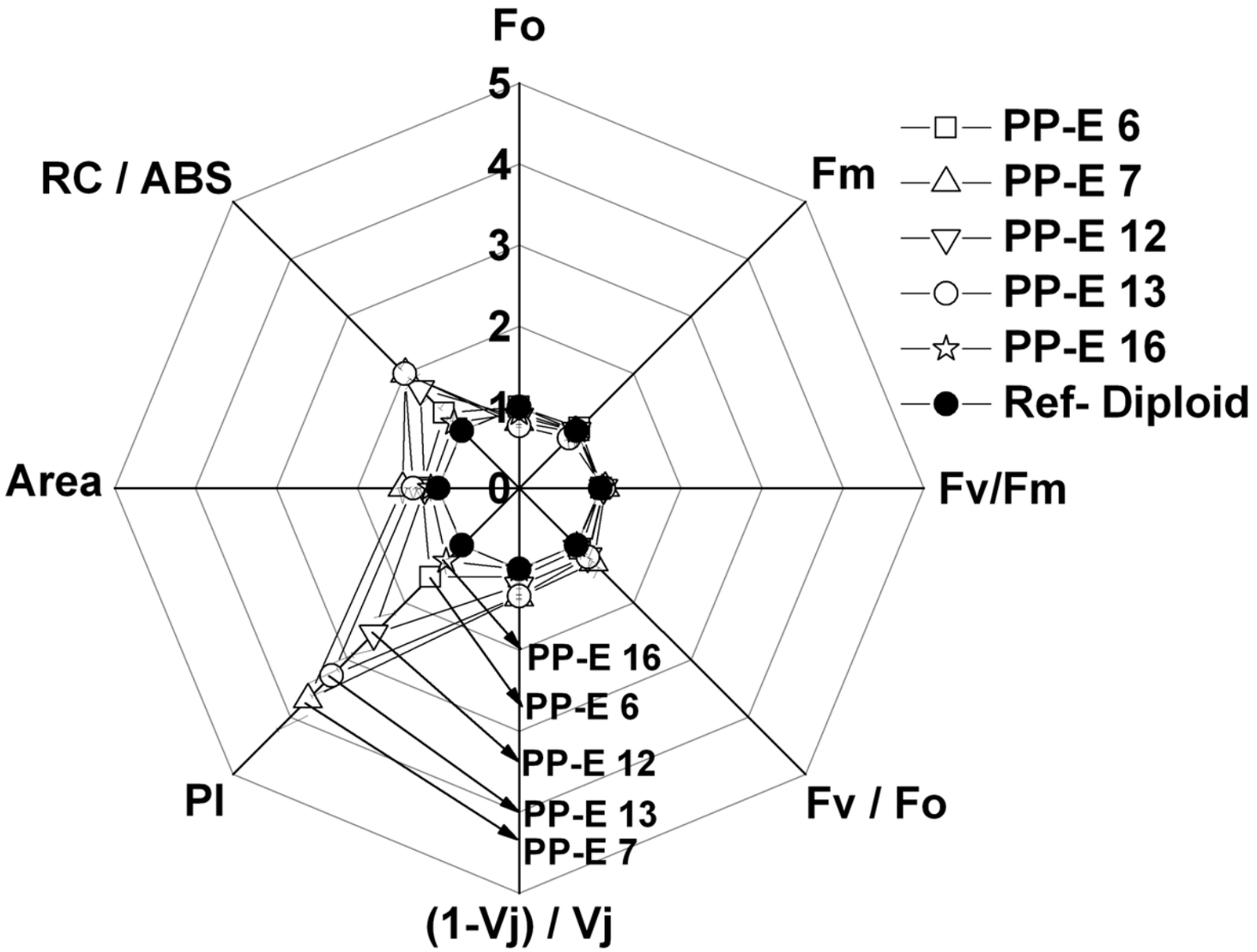

Figure 11. Spider plot of chlorophyll fluorescence parameters deduced from OJIP fast kinetics measurements. The figure shows the values of initial (F_o) and maximal (F_m) fluorescence levels; the F_v/F_m and the F_v/F_o (maximal PSII quantum yield) ratios, the $(1-V_j)/V_j$ parameter where $V_j = (F_{2ms} – F_o)/F_v$); the performance index (PI), the Area parameter, as well as the RC/ABS measured on $5^{th}/6^{th}$ young fully developed leaves. The data are shown for the tetraploid lines (*open symbols*) after normalization to respective value obtained in the diploid line (*closed symbol*). Data are mean ± SE of six to seven independent green house grown plants per genotype.

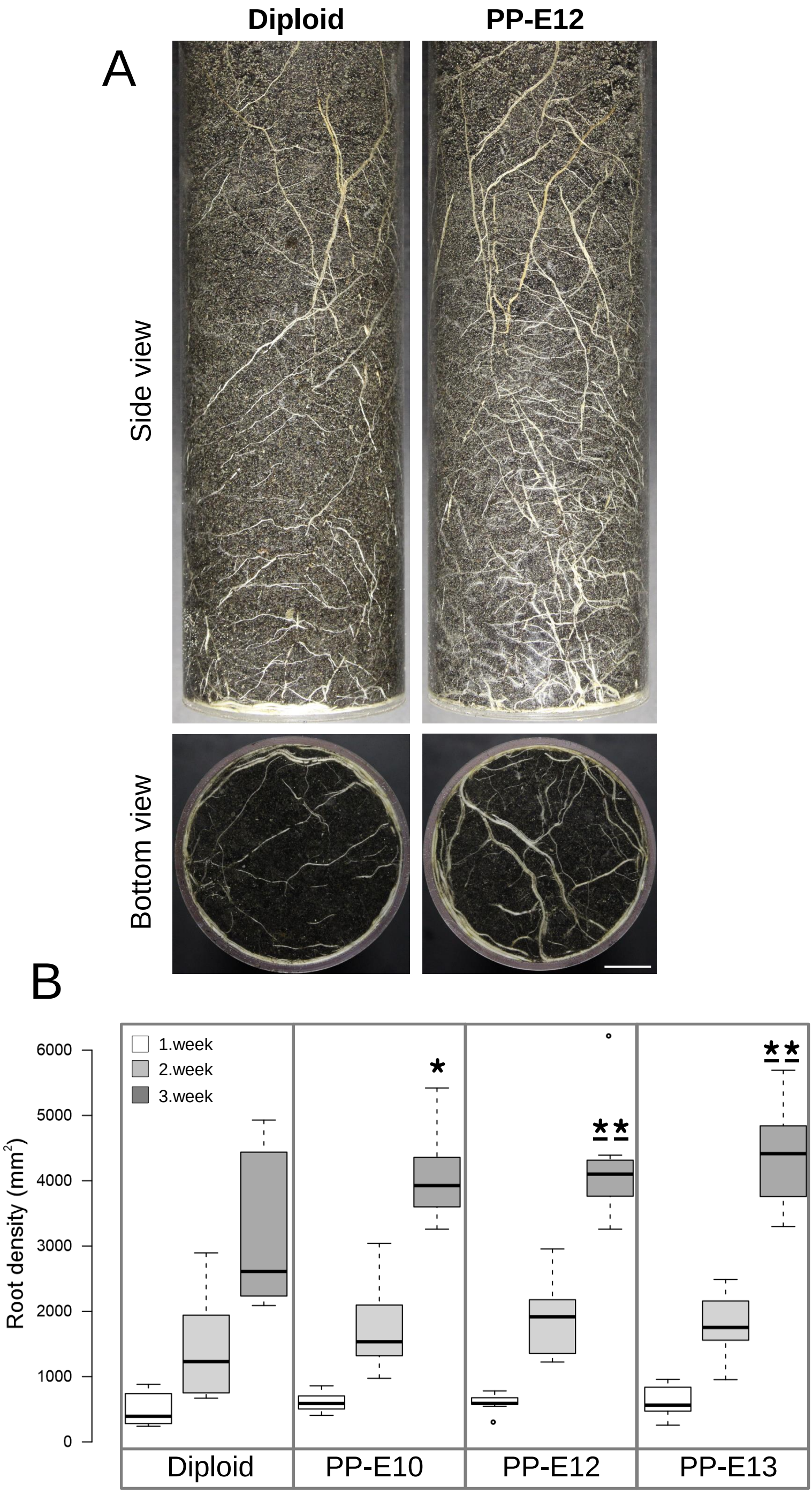

Figure 12. Significant stimulation of root development after duplication of genome size of energy willow. A, Side and bottom view of roots from the diploid and the tetraploid (PP-E12) plants grown in soil in transparent wall plexiglass columns. Digital images were taken at the third week of cultivation. Scale bar is 2 cm for all images. B, Total surface area (in mm^2) occupied by white pixels was used to monitor root biomass growth to compare diploid and tetraploid willow plants during the early development. Boxplot center lines show the medians; box limits indicate the 25th and 75th percentiles; whiskers extend 1.5 times the interquartile range from the 25th and 75th percentiles, outliers are represented by dots. Based on Welch's *t*-test, statistically significant events compared to diploids are indicated as **P<0.05 and *P<0.1. Underlined asterisks indicate the level of significance based on post-hoc comparisons made with the Tukey's HSD test. n = 10 sample points.

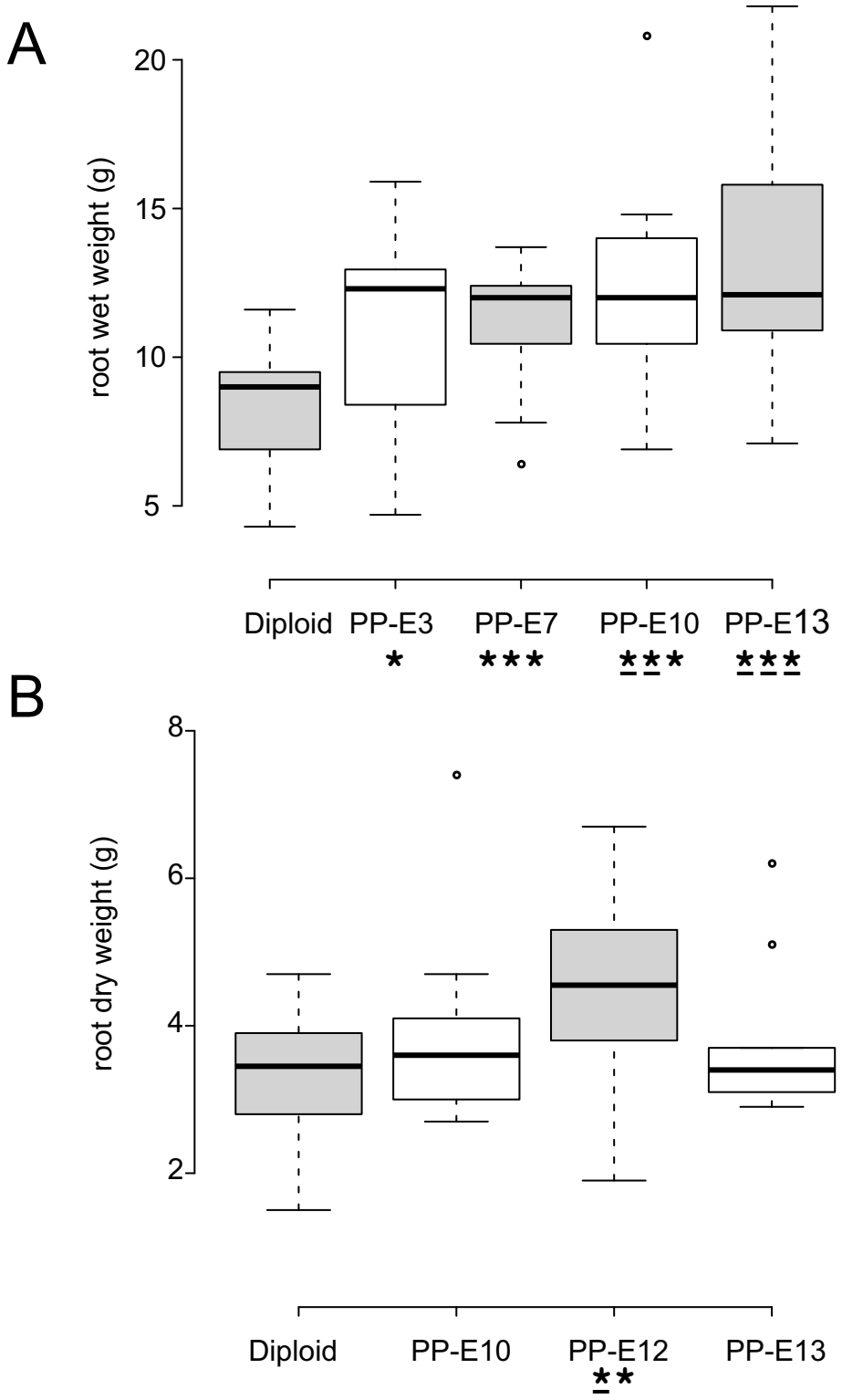

Figure 13. Autotetraploidization resulted in energy willow genotypes with increased root biomass. A, Experiment 1: Plants from tetraploid genotypes developed significantly more root than the control diploid ones based on fresh weight measurements (g/plant, n=10). B, Experiment 2: Increased root biomass of tetraploid willow genotypes as compared to diploid plants based on dry weight measurements (g/plant, n=10). Boxplot center lines show the medians; box limits indicate the 25th and 75th percentiles; whiskers extend 1.5 times the interquartile range from the 25th and 75th percentiles, outliers are represented by dots. Based on Welch's *t*-test, statistically significant events compared to diploids are indicated below the sample labels as *** P<0.01, ** P<0.05 and * P<0.12. Underlined asterisks indicate the level of significance based on post-hoc comparisons made with the Tukey's HSD test.

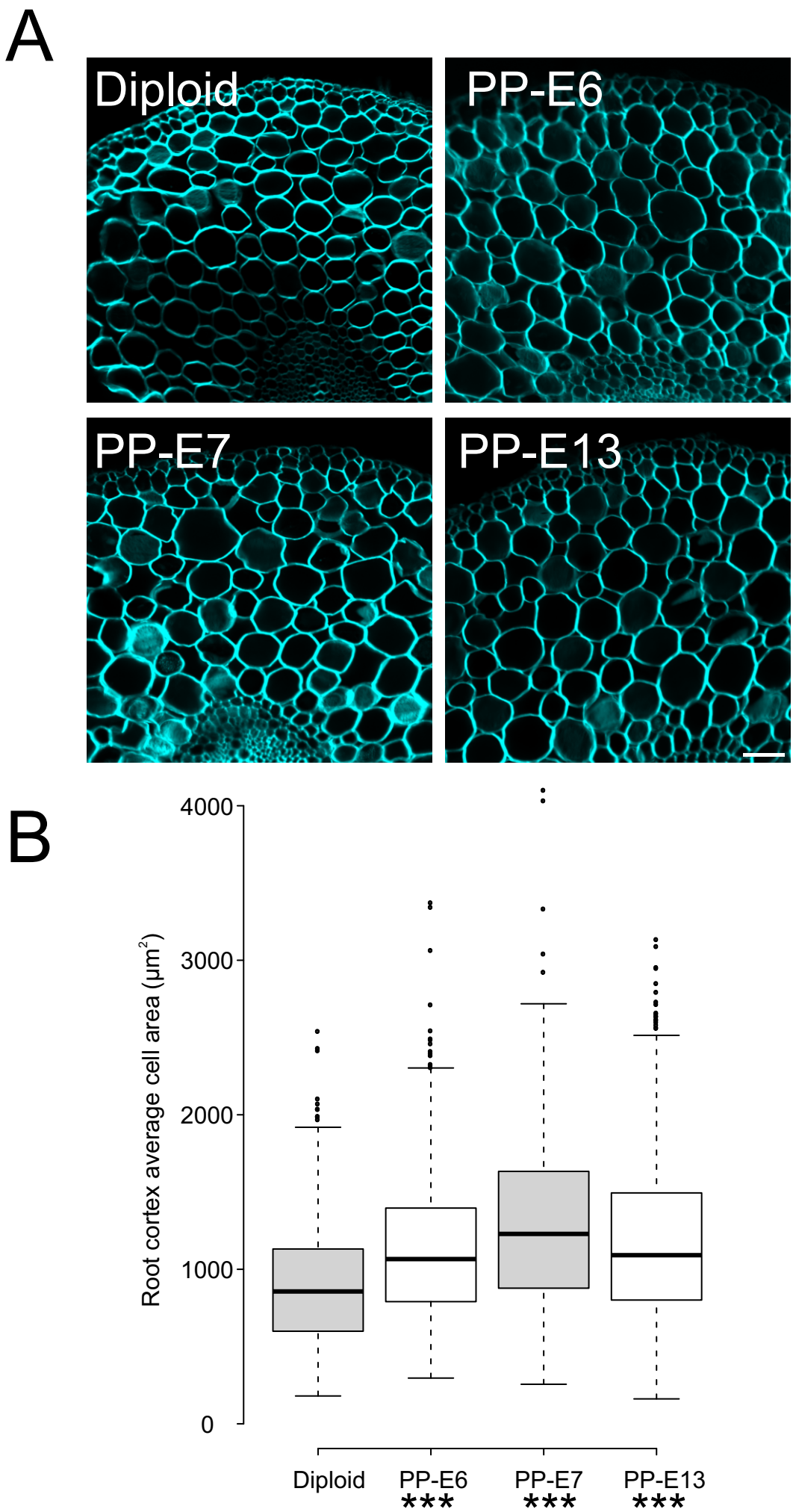

Figure 14. Differences in root anatomy detected between diploid and tetraploid willow plants. A, Calcofluor white stained, hand sectioned roots (from maturation zone) of diploid and tetraploid plants were imaged using confocal laser scanning microscope. Note the larger cortical cells of the tetraploid samples. Scale bar is 50µm for all images. B, Cortical cells of diploid and tetraploid roots were manually traced on hand-sectioned material using Olympus Fluoview software and average cross-sectional areas of cortical cells were calculated and plotted for diploid and tetraploid samples (n>362). Boxplot center lines show the medians; box limits indicate the 25th and 75th percentiles; whiskers extend 1.5 times the interquartile range from the 25th and 75th percentiles, outliers are represented by dots. Statistically significant events (based on both Welch's *t*-test and Tukey's HSD post hoc test) compared to diploids are indicated below the sample labels as *** P<0.01.

Parsed Citations

Alonso-Ramírez A, Rodríguez D, Reyes D, Jiménez JA, Nicolás G, López-Climent M, Gómez-Cadenas A, Nicoás C. (2009) Evidence for a role of gibberellins in salicylic acid-modulated early plant responses to abiotic stress in Arabidopsis seeds. Plant Physiol 150: 1335-1344

Pubmed: Author and Title
CrossRef: Author and Title
Google Scholar: Author Only Title Only Author and Title

Baker NR (2008) Chlorophyll fluorescence: a probe of photosynthesis in vivo. Annu Rev Plant Biol 59: 89-113

Pubmed: Author and Title
CrossRef: Author and Title
Google Scholar: Author Only Title Only Author and Title

Barcaccia G, Meneghetti S, Albertini E, Triest L, Lucchin M (2003) Linkage mapping in tetraploid willows: segregation of molecular markers and estimation of linkage phases support an allotetraploid structure for Salix alba x Salix fragilis interspecific hybrids. Heredity 90(2): 169-80

Pubmed: Author and Title
CrossRef: Author and Title
Google Scholar: Author Only Title Only Author and Title

Blakesley DA, Allen A, Pellny TK, Robersts AV (2002) Natural and induced polyploidy in Acacia dealbata Link. and Acacia mangium Willd. Ann Bot 90: 391-398

Pubmed: Author and Title
CrossRef: Author and Title
Google Scholar: Author Only Title Only Author and Title

Browse J (2009) Jasmonate passes muster: A receptor and targets for the defense hormone. Annu Rev Plant Biol 60: 183-205.

Pubmed: Author and Title
CrossRef: Author and Title
Google Scholar: Author Only Title Only Author and Title

Cai X, Kang XY (2011) In vitro tetraploid induction from leaf explants of Populus pseudo-simonii Kitag. Plant Cell Rep 30:1771-1778

Pubmed: Author and Title
CrossRef: Author and Title
Google Scholar: Author Only Title Only Author and Title

Camarero JJ, Palacio S, G. Montserrat-Marti G (2013) Contrasting seasonal overlaps between primary and secondary growth are linked to wood anatomy in Mediterranean sub-shrubs. Plant Biol 15: 798-807

Pubmed: Author and Title
CrossRef: Author and Title
Google Scholar: Author Only Title Only Author and Title

Cseri A, Sass L, Törjék O, Pauk J, Vass I, Dudits D (2013) Monitoring drought responses of barley genotypes with semi-robotic phenotyping platform and association analysis between recorded traits and allelic variants of some stress genes. Australian Journal of Crop Science 7:1560-1570

Pubmed: Author and Title
CrossRef: Author and Title
Google Scholar: Author Only Title Only Author and Title

Coate JE, Luciano AK, Seralathan V, Minchew KJ, Owens TG, Doyle JJ (2012) Anatomical, biochemical, and photosynthetic responses to recent allopolyploidy in Glycine dolichocarpa (Fabaceae). Am J Bot 99:55-67.

Pubmed: Author and Title
CrossRef: Author and Title
Google Scholar: Author Only Title Only Author and Title

Cortleven A, Schmülling T (2015) Regulation of chloroplast development and function by cytokinin. J Exp Bot. 66:4999-5013

Pubmed: Author and Title
CrossRef: Author and Title
Google Scholar: Author Only Title Only Author and Title

Cunniff J, Cerasuolo M (2011) Lighting the way to willow biomass production. J Sci Food Agric 91: 1733-1736

Pubmed: Author and Title
CrossRef: Author and Title
Google Scholar: Author Only Title Only Author and Title

De Lojo J, Di Benedetto A (2014) Biomass accumulation and leaf shape can be modulated by an exogenous spray of 6-benzylaminopurine in the ornamental foliage plant, Monstera deliciosa (Liebm.) J Horticultural Sciences, Biotechnology 89: 136-140

Pubmed: Author and Title
CrossRef: Author and Title
Google Scholar: Author Only Title Only Author and Title

Desotgiu R, Pollastrini M, Cascio C, Giacomo Gerosa G, Riccardo Marzuoli R, Bussotti F (2012) Chlorophyll a fluorescence analysis along a vertical gradient of the crown in a poplar (Oxford clone) subjected to ozone and water stress. Tree Physiol 32: 976-986

Pubmed: Author and Title
CrossRef: Author and Title
Google Scholar: Author Only Title Only Author and Title

Didi V, Jackson P, Hejatko J (2015) Hormonal regulation of secondary cell wall formation. J Exp Bot 66: 5015-5027
Pubmed: Author and Title
CrossRef: Author and Title
Google Scholar: Author Only Title Only Author and Title

Dobrev P, Kamínek M (2002) Fast and efficient separation of cytokinins from auxin and abscisic acid and their purification using mixed-mode solid-phase extraction. J of Chromatography A 950: 21-29
Pubmed: Author and Title
CrossRef: Author and Title
Google Scholar: Author Only Title Only Author and Title

Dobrev PI, Vanková R (2012) Quantification of abscisic acid, cytokinin, and auxin content in salt-stressed plant tissues. Methods in Molecular Biology 913: 251-261
Pubmed: Author and Title
CrossRef: Author and Title
Google Scholar: Author Only Title Only Author and Title

Dorn RD (1976) A synopsis of American Salix. Can J Bot 54: 2769-2789
Pubmed: Author and Title
CrossRef: Author and Title
Google Scholar: Author Only Title Only Author and Title

Dubouzet JG, Strabala TJ, Wagner A (2013) Potential transgenic routes to increase tree biomass. Plant Science 212: 72- 101
Pubmed: Author and Title
CrossRef: Author and Title
Google Scholar: Author Only Title Only Author and Title

Elias AA, Busov VB, Kosola KR, Ma C, Etherington E, Shevchenko O, Gandhi H, Pearce DW, Rood SB, Strauss SH (2012) Green revolution trees: semidwarfism transgenes modify gibberellins, promote root growth, enhance morphological diversity, and reduce competitiveness in hybrid Poplar. Plant Physiol 160: 1130-1144
Pubmed: Author and Title
CrossRef: Author and Title
Google Scholar: Author Only Title Only Author and Title

Eriksson ME, Israelsson M, Olsson O, Moritz T (2000) Increased gibberellin biosynthesis in transgenic trees promotes growth, biomass production and xylem fiber length. Nat Biotechnol 18: 784-788
Pubmed: Author and Title
CrossRef: Author and Title
Google Scholar: Author Only Title Only Author and Title

Ewald D, Ulrich K, Naujoks G, Schöder MB (2009) Induction of tetraploid poplar and black locust plants using colchicine: chloroplast number as an early marker for selecting polyploids in vitro. Plant Cell Tissue Organ Cult 99: 353-357
Pubmed: Author and Title
CrossRef: Author and Title
Google Scholar: Author Only Title Only Author and Title

Fariduddin Q, Hayat S, Ahmad A (2003) Salicylic acid influences net photosynthetic rate, carboxylation efficiency, nitrate reductase activity, and seed yield in Brassica juncea. Photosynthetica 41: 281-284.
Pubmed: Author and Title
CrossRef: Author and Title
Google Scholar: Author Only Title Only Author and Title

Fehér-Juhász E, Majer P, Sass L, Lantos Cs, Csiszár L, Turóczy Z, Mihály R, Mai A, Horváth GV, Vass I, Dudits D, Pauk J (2014) Phenotyping shows improved physiological traits and seed yield of transgenic wheat plants expressing the alfalfa aldose reductase under permanent drought stress. Acta Physiol Plant 36: 663-673
Pubmed: Author and Title
CrossRef: Author and Title
Google Scholar: Author Only Title Only Author and Title

Galbraith DW, Harkins KR, Maddox JM, Ayres NM, Sharma DP, Firoozabady E (1983) Rapid flow cytometric analysis of the cell cycle in intact plant tissues. Science 220: 1049-1051
Pubmed: Author and Title
CrossRef: Author and Title
Google Scholar: Author Only Title Only Author and Title

Genty B, Briantais JM, Baker NR (1989) The relationship between the quantum yield of photosynthetic electron transport and quenching of chlorophyll fluorescence. Biochim Biophys Acta 990: 87-92
Pubmed: Author and Title
CrossRef: Author and Title
Google Scholar: Author Only Title Only Author and Title

Golzarian MR, Frick RA, Rajendran K, Berger B, Roy S, Tester M, Lun DS (2011). Accurate inference of shoot biomass from high-throughput images of cereal plants. Plant Methods 7: 2
Pubmed: Author and Title
CrossRef: Author and Title
Google Scholar: Author Only Title Only Author and Title

Gou J, Strauss SH, Tsai CJ, Fang K, Chen Y, Jiang X, Busov VB (2010) Gibberellins regulate lateral root formation in Populus through interactions with auxin and other hormones. Plant Cell 22: 623-639
Pubmed: Author and Title

CrossRef: Author and Title
Google Scholar: Author Only Title Only Author and Title

Gou J, Ma C, Kadmiel M, Gai Y, Strauss S, Jiang X, Busov V (2011) Tissue specific expression of Populus C19 GA 2-oxidases differentially regulate above- and below-ground biomass growth through control of bioactive GA concentrations. New Phytol 192: 626-639
Pubmed: Author and Title
CrossRef: Author and Title
Google Scholar: Author Only Title Only Author and Title

Griffin AR, Chi NQ, Harbard JL, Son DH, Harwood CE, Price A, Vuong TD, Anthony Koutoulis A, Thinh HH (2015) Breeding polyploid varieties of tropical acacias: progress and prospects. Southern Forests 2015: 1-10
Pubmed: Author and Title
CrossRef: Author and Title
Google Scholar: Author Only Title Only Author and Title

Harbard JL, Griffin AR, Foster S, Brooker C, Kha LD, Koutoulis A (2012) Production of colchicine-induced autotetraploids as a basis for sterility breeding in Acacia mangium Willd. Forestry 85: 3427-3436
Pubmed: Author and Title
CrossRef: Author and Title
Google Scholar: Author Only Title Only Author and Title

Hartmann A, Czauderna T, Hoffmann R, Stein N, Schreiber F (2011) HTPheno: an image analysis pipeline for high-throughput plant phenotyping. BMC Bioinformatics 12: 148
Pubmed: Author and Title
CrossRef: Author and Title
Google Scholar: Author Only Title Only Author and Title

Huang JG, Deslauriers A, Rossi S (2014) Xylem formation can be modeled statistically as a function of primary growth and cambium activity. New Phytol 203: 831-841
Pubmed: Author and Title
CrossRef: Author and Title
Google Scholar: Author Only Title Only Author and Title

Jacobsen S-E, Rosenqvist E, Bendevis M, PrometheusWiki contributors (2012) Chlorophyll extraction with Dimethylformamide DMF. In: PrometheusWiki. http://prometheuswiki.publish.csiro.au/tikicitation.php?page=Chlorophyll%20extraction%20with%20Dimethylformamide%20DMF
Pubmed: Author and Title
CrossRef: Author and Title
Google Scholar: Author Only Title Only Author and Title

Jiang X, Li H, Wang T, Peng C, Wang H, Wu H, Wang X (2012) Gibberellin indirectly promotes chloroplast biogenesis as a means to maintain the chloroplast population of expanded cells. Plant J 72: 768-780
Pubmed: Author and Title
CrossRef: Author and Title
Google Scholar: Author Only Title Only Author and Title

Karp A, Hanley SJ, Trybush SO, Macalpine W, Pei M, Shield I (2011) Genetic improvement of willow for bioenergy and biofuels. J Integr Plant Biol 53(2): 151-165
Pubmed: Author and Title
CrossRef: Author and Title
Google Scholar: Author Only Title Only Author and Title

Klughammer C, Schreiber U (1994) An improved method, using saturating light pulses, for the determination of photosystem I quantum yield via P700+-absorbance changes at 830 nm. Planta 192: 261-268
Pubmed: Author and Title
CrossRef: Author and Title
Google Scholar: Author Only Title Only Author and Title

Kubota HF, Yoshimura Y (2002) Estimation of photosynthetic activity from the electron transport rate of photosystem 2 in film-sealed leaf of sweet potato, Ipomoea batatas Lam. Photosynthetica 40: 337-341
Pubmed: Author and Title
CrossRef: Author and Title
Google Scholar: Author Only Title Only Author and Title

Li WD, Biswas DK, Xu H, Xu CQ, Wang XZ, Liu JK, Jiang GM (2009) Photosynthetic responses to chromosome doubling in relation to leaf anatomy in Lonicera japonica subjected to water stress. Funct Plant Biol 36: 783-792
Pubmed: Author and Title
CrossRef: Author and Title
Google Scholar: Author Only Title Only Author and Title

Licausi F, Masaru Ohme-Takagi MO, Perata P (2013) APETALA2/Ethylene Responsive Factor (AP2/ERF) transcription factors: mediators of stress responses and developmental programs. New Phytol 199: 639-649
Pubmed: Author and Title
CrossRef: Author and Title
Google Scholar: Author Only Title Only Author and Title

Lu S, Lu X, ZhaoW, Liu Y, Wang Z, Omasa K (2015) Comparing vegetation indices for remote chlorophyll measurement of white poplar and Chinese elm leaves with different adaxial and abaxial surfaces. PMID: 26034132, J Exp Bot doi:10.1093/jxb/erv270
Pubmed: Author and Title

CrossRef: Author and Title
Google Scholar: Author Only Title Only Author and Title

Marmiroli M, Pietrini F, Maestri E, Zacchini M, Marmiroli N, Massacci A (2011) Growth, physiological and molecular traits in Salicaceae trees investigated for phytoremediation of heavy metals and organics. Tree Physiol 31: 1319-1334
Pubmed: Author and Title
CrossRef: Author and Title
Google Scholar: Author Only Title Only Author and Title

Matsumoto-Kitano M, Kusumoto T, Tarkowski P, Kinoshita-Tsujimura K, Vaclavikova K, Miyawaki K, Kakimoto T (2008) Cytokinins are central regulators of cambial activity. Proc Natl Acad Sci U S A 105: 20027-20031
Pubmed: Author and Title
CrossRef: Author and Title
Google Scholar: Author Only Title Only Author and Title

Mu HZ, Liu ZJ, Lin L, Li HY, Jiang J, Liu GF (2012) Transcriptomic analysis of phenotypic changes in birch (Betula platyphylla) autotetraploids. Int J Mol Sci 13: 13012-13029
Pubmed: Author and Title
CrossRef: Author and Title
Google Scholar: Author Only Title Only Author and Title

Mulkey SS, Smith M (1988) Measurement of photosynthesis by Infra Red Gas Analysis. In CT Lange ed., Bioinstrumentation, Publication of the American Biology Teachers Association, pp 79-84
Pubmed: Author and Title
CrossRef: Author and Title
Google Scholar: Author Only Title Only Author and Title

Murashige T, Skoog F (1962) A revised medium for rapid growth and bio-assays with tobacco tissue cultures. Physiol Plant 15(3): 473-497.
Pubmed: Author and Title
CrossRef: Author and Title
Google Scholar: Author Only Title Only Author and Title

Nelissen H, Rymen B, Jikumaru Y, Demuynck K, Lijsebettens MV, Kamiya Y, Inze D, Beemster GTS (2012) A local maximum in gibberellin levels regulates maize leaf growth by spatial control of cell division. Curr Biol 22: 1183-1187
Pubmed: Author and Title
CrossRef: Author and Title
Google Scholar: Author Only Title Only Author and Title

Németh AV, Dudits D, Molnár-Láng M, Linc G (2013) Molecular cytogenetic characterisation of Salix viminalis L. using repetitive DNA sequences. J Appl Genet 54: 265-269
Pubmed: Author and Title
CrossRef: Author and Title
Google Scholar: Author Only Title Only Author and Title

Newsholme C (1992) Willows, the Genus Salix. Timber Press, Portland, Oregon, USA.
Pubmed: Author and Title
CrossRef: Author and Title
Google Scholar: Author Only Title Only Author and Title

Ohashi-Ito K, Saegusa M, Iwamoto K, Oda Y, Katayama H, Kojima M, Sakakibara H, Fukuda H (2014) A bHLH Complex Activates Vascular Cell Division via Cytokinin Action in Root Apical Meristem. Current Biology 24: 2053-2058
Pubmed: Author and Title
CrossRef: Author and Title
Google Scholar: Author Only Title Only Author and Title

Pacifici E, Polverari L, Sabatini S (2015) Plant hormone cross-talk: the pivot of root growth. J Exp Bot 66: 1113-1121
Pubmed: Author and Title
CrossRef: Author and Title
Google Scholar: Author Only Title Only Author and Title

Quinn GP and Keough MJ (2002) Experimental Design and Data Analysis for Biologists, Cambridge Univeristy Press, Cambridge, p49.

Rao G, Sui J, Zeng Y, He C, Zhang J (2015) Genome-wide analysis of the AP2/ERF gene family in Salix arbutifolia. FEBS Open Bio (5): 132-137
Pubmed: Author and Title
CrossRef: Author and Title
Google Scholar: Author Only Title Only Author and Title

Ruxton GD (2006). The unequal variance t-test is an underused alternative to Student's t-test and the Mann-Whitney U test. Behavioral Ecology 17: 688-690.
Pubmed: Author and Title
CrossRef: Author and Title
Google Scholar: Author Only Title Only Author and Title

Ruzicka K, Ursache R, Hejatko J, Helariutta Y (2015) Xylem development - from the cradle to the grave. New Phytologist 207: 519-535
Pubmed: Author and Title
CrossRef: Author and Title
Google Scholar: Author Only Title Only Author and Title

Särkilahti E and Valanne T (1990) Induced polyploid in Betula. Silva Fennica 24:227-234
Pubmed: Author and Title
CrossRef: Author and Title
Google Scholar: Author Only Title Only Author and Title

Serapiglia MJ, Gouker FE, Smar LB (2014) Early selection of novel triploid hybrids of shrub willow with improved biomass yield relative to diploids. BMC Plant Biol 14: 74-86
Pubmed: Author and Title
CrossRef: Author and Title
Google Scholar: Author Only Title Only Author and Title

Strasser RJ, Tsimilli-Michael M, Srivastava A (2004) Analysis of the fluorescence transient. In G.C. Papageorgiou and Govindjee, eds, Advances in Photosynthesis and Respiration Series. Chlorophyll Fluorescence: a Signature of Photosynthesis. Springer, Dordrecht, The Netherlands, pp 321-362
Pubmed: Author and Title
CrossRef: Author and Title
Google Scholar: Author Only Title Only Author and Title

Spitzer M, Wildenhain J, Rappsilber J, Tyers M. (2014) BoxPlotR: a web tool for generation of box plots. Nat Methods. 11:121-122
Pubmed: Author and Title
CrossRef: Author and Title
Google Scholar: Author Only Title Only Author and Title

Strasser RJ, Srivastava A, Tsimilli-Michael M (2000) The fluorescence transient as a tool to characterize and screen photosynthetic samples. In Yunus M, Pathre UV, eds, Probing photosynthesis: Mechanisms regulation and adaptation. Taylor & Francis, New York, pp 443-480
Pubmed: Author and Title
CrossRef: Author and Title
Google Scholar: Author Only Title Only Author and Title

Suda Y, Argus GV (1968) Chromosome numbers of some North American Salix. Brittonia 20: 191-197
Pubmed: Author and Title
CrossRef: Author and Title
Google Scholar: Author Only Title Only Author and Title

Sugiyama SI (2005) Polyploidy and cellular mechanisms changing leaf size: comparison of diploid and autotetraploid populations in two species of Lolium. Ann Bot 96: 931-938
Pubmed: Author and Title
CrossRef: Author and Title
Google Scholar: Author Only Title Only Author and Title

Tackenberg O (2007) A new method for non-destructive measurement of biomass, growth rates, vertical biomass distribution and dry matter content based on digital image analysis. Annals of Botany 99:777-783
Pubmed: Author and Title
CrossRef: Author and Title
Google Scholar: Author Only Title Only Author and Title

Taiz L, Zeiger E (2010) Plant Physiology, Fifth Edition. Sinauer Associates, Inc. Sunderland, MA, USA
Pubmed: Author and Title
CrossRef: Author and Title
Google Scholar: Author Only Title Only Author and Title

Taneda H, Terashima I (2012) Co-ordinated development of the leaf midrib xylem with the lamina in Nicotiana tabacum. Ann Bot 110: 35-45
Pubmed: Author and Title
CrossRef: Author and Title
Google Scholar: Author Only Title Only Author and Title

Tang ZQ, Chen DL, Song ZJ, He YC, Cai DT (2010) In vitro induction and identification of tetraploid plants of Paulownia tomentosa. Plant Cell Tissue Organ Cult 102: 213-220
Pubmed: Author and Title
CrossRef: Author and Title
Google Scholar: Author Only Title Only Author and Title

Vicente MRS, Plasencia J (2011) Salicylic acid beyond defence: its role in plant growth and development. J Exp Bot 62: 3321-3338
Pubmed: Author and Title
CrossRef: Author and Title
Google Scholar: Author Only Title Only Author and Title

Walter A, Liebisch F, Hund A (2015) Plant phenotyping: from bean weighing to image analysis. Plant Methods 11:14
Pubmed: Author and Title
CrossRef: Author and Title
Google Scholar: Author Only Title Only Author and Title

Wang J, Shi L, Song S, Tian J, Kang X (2013) Tetraploid production through zygotic chromosome doubling in Populus. Silva Fennica vol. 47 no. 2 article id 932. 12 p. ISSN-L 0037-5330 | ISSN 2242-4075 (Online)
Pubmed: Author and Title
CrossRef: Author and Title
Google Scholar: Author Only Title Only Author and Title

Wang Z, Wang M, Liu L, Meng F (2013) Physiological and proteomic responses of diploid and tetraploid black locust (Robinia pseudoacacia L.) subjected to salt stress. Int. J. Mol. Sci. 14:20299-20325
Pubmed: Author and Title
CrossRef: Author and Title
Google Scholar: Author Only Title Only Author and Title

Warner DA. Edwards GE (1989) Effects of polyploidy on photosynthetic rates, photosynthetic enzymes, contents of DNA, chlorophyll, and sizes and numbers of photosynthetic cells in the C4 dicot Atriplex confertifolia. Plant Physiol 91: 1143-1151
Pubmed: Author and Title
CrossRef: Author and Title
Google Scholar: Author Only Title Only Author and Title

Warner DA, Edwards GE (1993) Effects of polyploidy on photosynthesis. Photosynth Res. 35: 135-47.
Pubmed: Author and Title
CrossRef: Author and Title
Google Scholar: Author Only Title Only Author and Title

Wellburn AR (1994) The spectral determination of chlorophylls a and b, as well as total carotenoids, using various solvents with spectrophotometers of different resolution. Journal of Plant Physiology 144: 307-313.
Pubmed: Author and Title
CrossRef: Author and Title
Google Scholar: Author Only Title Only Author and Title

Ye ZH, Zhong R (2015) Molecular control of wood formation in trees. Journal of Experimental Botany 66: 4119-4131
Pubmed: Author and Title
CrossRef: Author and Title
Google Scholar: Author Only Title Only Author and Title

Zivcak M, Brestic M, Olsovska K, Slamka P (2008) Performance index as a sensitive indicator of water stress in Triticum aestivum L. Plant Soil Environ 54(4): 133-139
Pubmed: Author and Title
CrossRef: Author and Title
Google Scholar: Author Only Title Only Author and Title

Zurek G, Rybka K, Pogrzeba M, Krzyzak J, Prokopiuk K (2014) Chlorophyll a fluorescence in evaluation of the effect of heavy metal soil contamination on perennial grasses. PLoS One 9:e91475. doi:10.1371/journal.pone.0091475
Pubmed: Author and Title
CrossRef: Author and Title
Google Scholar: Author Only Title Only Author and Title